TECHNICAL REPORT

DEPARTMENT OF PHYSICS

UNIVERSITY OF CALIFORNIA

LOS ANGELES

CONTRACT RESEARCH

SPONSORED BY

OFFICE OF NAVAL RESEARCH

THE ABSORPTION OF SOUND

IN GAS MIXTURES

by

FRANK A. ANGONA

Technical Report No V

January, 1953

Submitted by

R.W. Leonard, Project Director

TABLE OF CONTENTS

I. INTRODUCTION

As a sound wave propagates through a polyatomic gas
the acoustic energy is found to diminish. This loss of en-
ergy is mainly attributed to the attenuation due to the vis-
cosity, the heat conduction, and the molecular relaxation of
the gas. For a large portion of the frequency spectrum,
the viscous and heat conduction effects are small compared
to the molecular attenuation. The source of molecular ab-
sorption of sound in a gas is a lag in adjustment between
the internal energy states of the molecules and their energy
of translation. During a condensation of a sound wave, the
temperature of the gas rises. This excess translational
energy causes some of the molecules to acquire a quantum of
energy which raises them to a higher internal energy state.
The molecules of a gas require on the average a certain
time to acquire and then lose their quanta of energy; this
time is known as the relaxation time of that particular
state.

Molecular absorption is dependent on the relative
values of the relaxation time and the period of the sound
wave. For low sonic frequencies, the period between con-
densations is long compared to the relaxation time and no
loss of acoustic energy occurs. For extremely high sonic

frequencies, the period between condensations is not of sufficient duration to permit much energy to be transferred to internal modes. Consequently, the loss of acoustic energy per wavelength is small. However, the absorption per cm is still appreciable due to the large number of wavelengths per cm. For those frequencies where the period is of the same order of magnitude as the relaxation time, a large loss in acoustic energy per wavelength will occur. Hence, one would expect the molecular attenuation per wavelength to be a maximum at intermediate frequencies and to become smaller as the frequency is either increased or decreased.

The relaxation time of a gas is dependent on the number of collisions per second and on the effectiveness of each collision. Since the rate of collision is proportional to the number of molecules present, the relaxation time can be controlled by the pressure of the gas. This pressure dependence can be used to adjust the relaxation time so that the maximum absorption of sound per wavelength will occur in any desired frequency range.

This dissertation is concerned with the measurement of the molecular absorption of sound in CO_2, in CS_2, and in C_2H_4O, and also in mixtures of these gases. The absorption of sound in gases can be measured by the interferometer method, the resonance sharpness method, the direct method, and the tube method. The latter method was chosen as it is readily adaptable to both frequency and pressure control;

it can be designed to use a relatively small sample of gas which simplifies the drying and purification problem, it can be made vacuum tight, and it can be designed to give a sufficiently strong signal for measuring the attenuation of gases which are highly absorptive.

II. HISTORICAL SURVEY OF ATTENUATION

The classical absorption of sound in a gas is caused by the viscosity and the heat conduction of the gas. This subject was first studied by Stokes and Kirchhoff. Lord Rayleigh[1] discusses the classical attenuation in detail and gives for the attenuation coefficient of the sound pressure

$$\alpha_c = \frac{\omega^2}{2a^3}\left[\mu' + \mu'' + \nu\left(1 - \frac{b^2}{a^2}\right)\right]$$

(1)

where

$$a = \left(\frac{\gamma p}{\rho}\right)^{1/2}$$ Laplace's sound velocity (adiabatic)

$$b = \left(\frac{p}{\rho}\right)^{1/2}$$ Newton's sound velocity (isothermal)

$$\nu = \frac{K}{C_v \rho}$$ Thermometric conductivity

$$\mu' = \frac{\mu}{\rho}$$ Kinematic shear viscosity

$$\mu'' = \frac{1}{3}\mu'$$ (for a perfect gas)

$$\omega = 2\pi f$$ Angular frequency

By including the above definitions and the equation of state for a perfect gas equation (1) can be written in a

form more usable for experimental work

$$\alpha_c = \frac{2\pi^2 R T}{a^3 M}\mu\left[\frac{4}{3} + \frac{K}{\mu C_v}\left(\frac{\gamma-1}{\gamma}\right)\right]\frac{f^2}{p} \tag{2}$$

where
- R = gas content
- T = temperature
- M = molecular weight of gas
- μ = viscosity
- K = Heat conductivity
- C_v = specific heat at constant volume
- γ = ratio of the specific heats
- f = accustic frequency
- p = gas pressure

The above expression will be discussed further in the section concerned with experimental results.

As far back as 1911, the measurements of Neklepajew[2] indicated that for air the absorption could not be explained entirely by viscosity and heat conduction. Later measurements by Abello[3] Grossman,[4] Pierce,[5] Rich and Pielemeier,[6] and Knudsen[7] gave further evidence that the classical absorption had to be modified. In the early part of this century, Jeans[8] developed a classical molecular theory which considered the lag in adjustment between the internal energy states of the molecules and their energy of translation. He indicated that this effect could explain the anomalous absorption observed in polyatomic gases. In 1920, Einstein[9] developed a theory for the dispersion of sound in partially dissociated gases. Although Einstein was primarily interested

in determining the rate of dissociation of a gas and not the dispersion of sound, his paper has been the foundation for other papers using the thermodynamical approach to the theory of sound absorption and dispersion in gases. In 1928, Herzfeld and Rice,[10] expanding the idea of Jeans, developed a theory for the absorption and dispersion of sound in gases. Kneser,[11] in 1931, following Einstein, developed a simplified theory assuming only the first vibrational state of the molecules to be activated. Kneser was able to explain the abnormal absorption of sound in air found by Knudsen. Bourgin,[12] using the methods of statistical mechanics, developed the Herzfeld and Rice theory into its present form. In his later papers,[13] he shows the Kneser theory is a special case of his more rigorous and more general treatment.

Since the early 1930s, a large number of experimental papers concerned with molecular absorption have been presented. Only those papers which are pertinent to this dissertation shall be mentioned. Leonard,[14] in 1939, measured the absorption of sound in CO_2 by the direct method. This method is concerned with the determination of the absorption as a function of distance. The reduction in sound pressure in excess of the inverse distance loss is the absorption due to the gas itself. In the following year, Fricke[15] measured the absorption of sound in five triatomic gases. He compared the sound pressure of pure nitrogen to that of various mixtures of nitrogen and the gas under test using a micro-

phone at a fixed distance from a sound source. In 1942, Frick[16] measured the absorption and dispersion of sound in CO_2 and N_2O and also in mixtures of each gas with nitrogen by the direct method.

III. THEORETICAL DISCUSSION

Molecular Absorption

Bourgin[13] has developed an expression for the sound absorption per wavelength for a mixture of two absorbing gases. As pointed out by Frick, the original paper contained some typographical errors causing the expression to be dimensionally incorrect. The corrected expression is

$$\mu = \frac{\frac{2\pi\omega R}{N}\left[\frac{AC_A}{\Sigma_A}\left(1+\frac{\omega^2}{\Sigma_B^2}\right) + \frac{BC_B}{\Sigma_B}\left(1+\frac{\omega^2}{\Sigma_A^2}\right)\right]}{\left[\begin{array}{l}C_\infty(C_\infty+R)\left(1+\frac{\omega^2}{\Sigma_A^2}\right)\left(1+\frac{\omega^2}{\Sigma_B^2}\right) + (2C_\infty+R)C_i + C_i^2 \\ + \frac{\omega^2}{N}(2C_\infty+R)\left(\frac{AC_A}{\Sigma_B^2} + \frac{BC_B}{\Sigma_A^2}\right) + \frac{\omega^2}{N^2}\left(\frac{AC_A}{\Sigma_B} + \frac{BC_B}{\Sigma_A}\right)^2\end{array}\right]} \tag{3}$$

where μ = intensity absorption coefficient per wavelength

ω = 2π times sound frequency

R = gas constant per mole.

N = number of molecules per unit volume of the mixture

A = number of molecules per unit volume of gas A

B = number of molecules per unit volume of gas B

C_A = vibrational specific heat per mole. for gas A

C_B = vibrational specific heat per mole. for gas B

C_1 = vibrational specific heat per mole. for the mixture

C_∞ = specific heat per mole of the mixture at infinite frequency

$\sum_A$ is proportional to the reciprocal of the relaxation time for gas A

$\sum_B$ is proportional to the reciprocal of the relaxation time for gas B

Frick has shown that by regrouping Bourgin's expression for $\sum_A$ and $\sum_B$ and making use of Boltzmann's Distribution Law, it is possible to write

$$\sum_A = \frac{1}{T_{10}^A}\left(1 + e^{-\frac{\theta_A}{T}}\right) \tag{4}$$

$$\sum_B = \frac{1}{T_{10}^B}\left(1 + e^{-\frac{\theta_A}{T}}\right) \tag{5}$$

where

T_{10}^A = Relaxation time for gas A

T_{10}^B = Relaxation time for gas B

θ_A = Characteristic temperature for gas A

θ_B = Characteristic temperature for gas B

The above equations assume only one mode of vibration to be active in sound absorption; hence, they cannot be used rigorously to calculate the relaxation time. However, for most gases the mode of vibration corresponding to the lowest characteristic temperature contributes a large percentage of the vibrational specific heat; consequently, it seems reasonable to calculate the relaxation time using this particular value of the characteristic temperature.

For the special case of a single absorbing gas,

$A = N$, $B = 0$, and $\Sigma_B = \infty$, equation (3) becomes

$$\mu = \frac{2\pi\omega R\, \Sigma_A C_A}{C_\infty(C_\infty + R)\left[\omega^2 + \Sigma_A\left(1 + \frac{C_A}{C_\infty}\right)\left(1 + \frac{C_A}{C_\infty + R}\right)\right]} \tag{6}$$

When equation (6) is plotted against the logarithm of the frequency a bell shaped curve results having a maximum absorption per wavelength

$$\mu_{max} = \frac{\pi R C_A}{\left[C_\infty(C_\infty + R)(C_\infty + C_A)(C_\infty + C_A + R)\right]^{1/2}} \tag{7}$$

at an angular frequency of

$$\omega_{max} = \Sigma_A\left[\left(1 + \frac{C_A}{C_\infty}\right)\left(1 + \frac{C_A}{C_\infty + R}\right)\right]^{1/2} \tag{8}$$

When equation (8) is substituted back in equation (6)

$$\mu = \frac{2\pi R C_A\, \omega\, \omega_{max}}{\left[C_\infty(C_\infty + R)(C_\infty + C_A)(C_\infty + C_A + R)\right]^{1/2}\left[\omega^2 + \omega_{max}^2\right]} \tag{9}$$

which is identical with the expression for the absorption per wavelength developed by Kneser.

Another special case of Bourgin's equations (3) is when the vibrational specific heats for each gas are small

compared to the specific heat of the mixture at infinite
frequency. (i.e. $\frac{HC_A}{NC_\infty} < 1$, $\frac{BC_B}{NC_\infty} < 1$). Under these
circumstances equation (3) reduces to

$$\mu = \frac{2\pi\omega R}{NC_\infty(C_\infty + R)}\left[\frac{\Sigma_A HC_A}{\omega^2 + \Sigma_A^2} + \frac{\Sigma_B BC_B}{\omega^2 + \Sigma_B^2}\right] \qquad (10)$$

This expression shows that the total absorption per wave-
length is the sum of the effects due to each gas independent-
ly.

Although for the gas mixtures used in this disserta-
tion the above approximations are not strictly valid, the
experimental results, which are discussed in a later section,
appear to be in approximate agreement with equation (10).

Determination of Specific Heat from Spectroscopic Data.

A check on the measured absorption coefficient can be
made by calculating the pertinent constants of the gas from
spectroscopic data. A reasonably accurate value of the spe-
cific heat can be obtained if one assumes the molecule acts
as a harmonic oscillator and the interaction between rota-
tion and vibration is negligible. The specific heat at
constant volume can be determined as follows:

$$C_v = x_T\left(\frac{1}{2}R\right) + x_R\left(\frac{1}{2}R\right) + C_{vib} \qquad (11)$$

where α_T = number of degrees of freedom for translation

α_R = number of degrees of freedom for rotation

C_{vib} = specific heat due to vibration

$$c_{vib} = \sum_{i=1}^{n} p_i \, P\left(\frac{\theta_i}{T}\right)$$

where p_i = multiplicity of the ith energy level

$P\left(\frac{\theta_i}{T}\right)$ = contribution to the specific heat due to the ith mode of vibration

The following paragraphs will be concerned with the explicit form of $P\left(\frac{\theta_i}{T}\right)$. The partition function for a single mode (V_i) of vibration can be written as

$$Q_{V_i} = \sum_{n=0}^{\infty} p_i \, e^{-\frac{n\theta_i}{T}}$$

where θ_i = characteristic temperature of the ith mode of vibration

The above notation is rather misleading with respect to the role of the multiplicity. When $p_i = 1$, the series representation of the partition function is

$$Q_{V_i} = 1 + e^{-\theta_i/T} + e^{-2\theta_i/T} + e^{-3\theta_i/T} + \cdots\cdots$$

However, for $p_i = 2$, the series is repeated and the resulting product gives

$$Q_{V_i} = 1 + 2e^{-\theta_i/T} + 3e^{-2\theta_i/T} + 4e^{-3\theta_i/T} + \cdots\cdots$$

From thermodynamics, the specific heat may be written as a function of the partition function

$$\left(C_{vib}\right)_i = R\frac{d}{dT}\left[T^2\frac{d}{dT}\ln Q_{v_i}\right]$$

(12)

$$\left(C_{vib}\right)_i = R\left[\frac{2T}{Q_{v_i}}\frac{dQ_{v_i}}{dT} - \left(\frac{T}{Q_{v_i}}\frac{dQ_{v_i}}{dT}\right)^2 + \frac{T^2}{Q_{v_i}}\frac{d^2Q_{v_i}}{dT^2}\right]$$

The above expression may be used to determine the contribution to the specific heat of any number of harmonics of a particular mode. If one is interested in the specific heat due to all the harmonics of a particular mode, the above expression for Q can be put in closed form.

$$Q_{v_i} = \sum_{n=0}^{\infty} p_i\, e^{-n\theta_i/T} = \frac{1}{\left(1 - e^{-\theta_i/T}\right)}p_i$$

When this expression for Q is put in equation (12) it becomes

$$\left(C_{vib}\right)_i = p_i\, R\left(\frac{\theta_i}{T}\right)^2 \frac{e^{-\theta_i/T}}{\left(1 - e^{-\theta_i/T}\right)^2}$$

(13)

which is the function $P\left(\frac{\theta_i}{T}\right)$ we set out to determine. The use of equations (12) and (13) will be demonstrated in the section on results.

Attenuation Due to the Tube

For many years tubes have been used as a means of producing and guiding plane acoustic waves. In 1868, Kirchhoff developed an expression for the attenuation of sound due to the thermal and viscous losses at the walls of the tube. In the notation of Rayleigh

$$\alpha_T = \left(\frac{\omega}{2}\right)^{1/2} \frac{\delta'}{a \, \Lambda} \tag{14}$$

where

$$\delta' = (\mu')^{1/2} + \left(\frac{a}{b} - \frac{b}{a}\right) \nu^{1/2}$$

$a = \left(\frac{\gamma P}{\rho}\right)^{1/2}$ Laplace's sound velocity (adiabatic)

$b = \left(\frac{P}{\rho}\right)^{1/2}$ Newton's sound velocity (isothermal)

$\mu' = \frac{\mu}{\rho}$ kinematic shear viscosity

$\nu = \frac{K}{C_v \rho}$ thermometric conductivity

$\Lambda =$ radius of the sound tube

Equation (14) can be written in a form more usable for experimental application

$$\alpha_T = \frac{(\pi \mu)^{1/2}}{\Lambda} \left[\frac{1}{\gamma^{1/2}} + \frac{\gamma-1}{\gamma} \left(\frac{K}{C_v \mu}\right)^{1/2} \right] \left(\frac{f}{P}\right)^{1/2} \tag{15}$$

where all symbols have the same meaning as for equation (2). Many investigations of the tube effect have been reported in

the literature.[17-22] The majority agree the Kirchhoff equation is correct as to dependence on the radius, frequency, and pressure; in addition, most of the investigators found the measured tube effect to be greater than that predicted by Kirchhoff's equation. This difference between the calculated and the observed attenuation ranges from a negligible amount to as much as 15%.

Since the tube method was employed for all attenuation measurements for this dissertation, the effect of the tube was of importance. An uncertainty in the tube effect ranging from 0% to 15% could cause an error in the attenuation per wavelength of as much as 4%. Consequently, it was decided to measure the tube effect. As can be seen from equation (15) both frequency and pressure may be used as parameters. Since the Kirchhoff theory is restricted to plane waves, the frequency is limited to those values below the cut-off frequency of the first non-plane mode. For a cylindrical tube the cut-off frequency for the first sloshing mode as given by Morse[23] is

$$\mathcal{V}_{/0} = \frac{.5861\ C}{2\ r} \tag{16}$$

where   C = velocity of sound in cm/sec
r = radius of the tube in cm

At atmospheric pressure and even at the upper limit of frequency, the magnitude of the tube attenuation is a relatively

small quantity and offers some difficulty in measuring. Consequently, the use of an apparatus in which pressure can be controlled is advantageous. All other factors being equal, a reduction of pressure by a factor of 100 gives a 10 fold increase in magnitude of the tube effect and a corresponding increase in accuracy of experimental measurement. The results of these measurements are discussed in the section on results.

IV. APPARATUS

The apparatus used for this investigation is shown in the photograph on page 18 and is also shown in schematic form in Figure 1. The speaker is moved with respect to the microphone by a magnet which surrounds the sound tube. The sound pressure is recorded as the distance between the speaker and the microphone is varied. The slope of this record yields the attenuation coefficient. In addition a measure of the sound velocity is simultaneously made by measuring the distance between points of equal phase. These measurements are repeated for various values of the sound frequency and the gas pressure. A detailed description of the various components of the apparatus is given below.

Speaker.

In order to use the tube method for measuring the absorption, either the speaker or the microphone must be of the movable type. The decision to allow the speaker to move eliminated the possibility of using a conventional speaker. Therefore, the design and development of a speaker small enough to fit inside a small bore tube was initiated. The desired properties for the speaker were: reasonable output from 2 to 10 kc without heating more than about 2° C, not over 1.60 cm in diameter, capable of moving freely
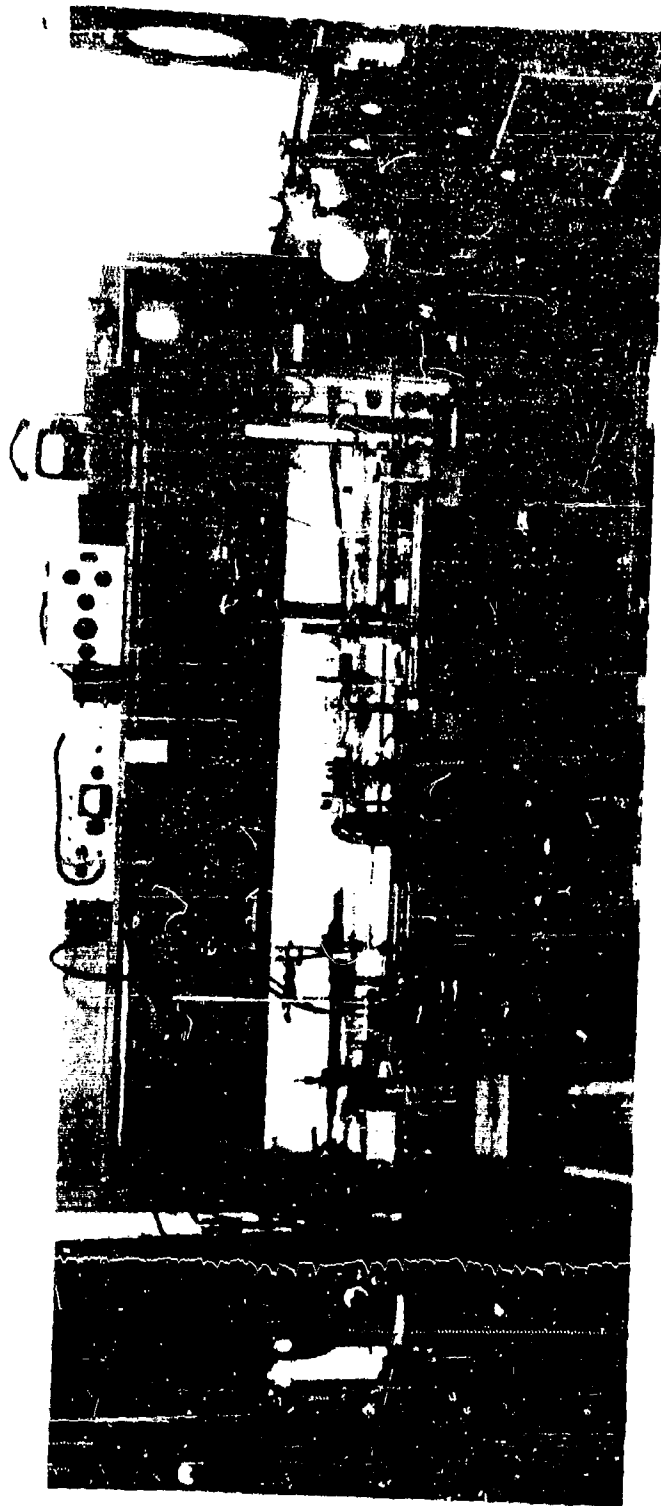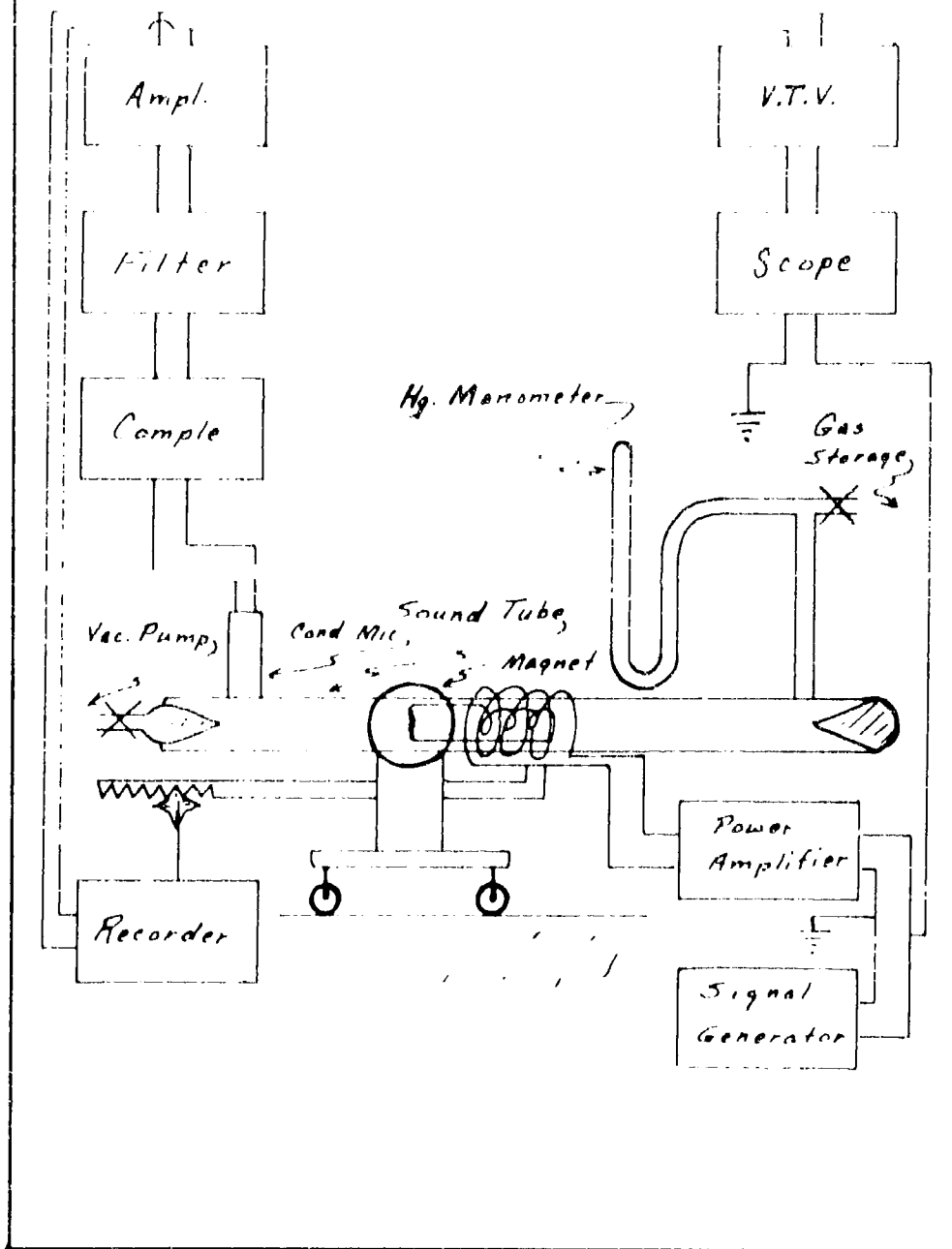
Fig. 1

inside a glass tube, mounted in a manner to avoid trans-
mitting mechanical vibration to the glass tube, made of a
material which would not react with the gases to be tested
or outgas in a vacuum, and coupled to a signal generator in
such a manner as to minimize electromagnetic radiation. The
speaker which finally evolved is of the ribbon type. The
ribbon is made of 1/4 mil aluminum foil. The foil is mounted
on the speaker housing by a tapered tefelon ring which fits
snugly around the front end of the speaker housing. The rib-
bon is corrugated to eliminate any chance of stretching as
the ring is pushed in place. Electrical energy is fed to
the foil by an air core transformer. The primary is a coil
of 115 turns of 16 gauge copper wire. The secondary consists
of 3 turns of 14 gauge copper wire. The secondary is mounted
at the rear of the speaker housing and at a sufficient dis-
tance from the foil to be out of the region of strong mag-
netic field. This was done so as to reduce any mechanical
vibration caused by the interaction of the magnetic field
with the current flowing through the transformer. A large
magnet carried on a cart which is guided by tracks running
parallel to the sound tube is used to supply the magnetic
field for the ribbon. The pole pieces of the magnet are two
pairs of truncated cones designed so as to concentrate the
magnetic field into two separate regions. The major field
is applied at the ribbon to interact with the current flow-
ing in the ribbon, thus causing it to vibrate and serve as

a sound source. The remainder of the magnetic field is
concentrated at a point 7/8 of an inch behind the ribbon.
At this point a steel pin 1/4 inch in diameter and approxi-
mately 0.6 inches long is mounted on the speaker housing and
in a direction parallel to the magnetic field. This serves
as a coupling between the speaker and the magnet which
causes the speaker to follow any movement of the magnet. The
speaker housing is made of glass to insure against outgassing
and any reaction with the gases to be tested. To permit
evacuation of the sound tube with the speaker in place and
also to eliminate any change in gas pressure when the speaker
is in motion, the speaker foil is allowed to fill only 2/3
of the cross-sectional area of the tube and the speaker hous-
ing is made in the shape of a hollow cylinder. To minimize
the transmission of vibration from the speaker to the glass
sound tube, rubber "O" rings with a tefelon cap are used to
support the speaker in the sound tube. The rubber serves as
a vibration insulator and the tefelon cap reduces the fric-
tional drag of the speaker on the glass sound tube. The
photograph on page 22 shows the speaker in its normal posi-
tion within the sound tube.

Microphone.

As all acoustic measurements were made on gases at
pressures much less than atmospheric, a problem arose as to
the best method of connecting a microphone to the sound tube.

A membrane between the microphone and the rarified gas in the sound tube was tried. However, the acoustic losses due to the poor impedance match were too great. To eliminate the need for a membrane, a special microphone was designed which served both as a sound pickup and as a window for the sound tube. The microphone is of the condenser type. The microphone head was made from a solid right cylinder of aluminum which was machined to give a diaphragm of .006 inch thickness. The head is threaded to fit a brass block which serves as a connector for the two sections of the sound tube and the microphone. All connections were designed to give a minimum change in cross-sectional area of the sound tube in order to reduce sound reflections from the microphone. The connections are sealed with Apiezon A black wax.

The backing plate was made adjustable. The spacing between the diaphragm and the backing plate was adjusted while the sound tube was evacuated to give approximately 14 $\mu\mu f$ capacitance. A standard 640 AA pre-amplifier is used in conjunction with the microphone. The compliance of the diaphragm is such that the microphone cuts off when the gas pressure in the sound tube approaches 300 mm of mercury. Although the sensitivity of the microphone is a function of pressure, no problem is encountered as only relative values of sound pressure at a fixed gas pressure are required for any particular determination of the attenuation coefficient.

Likewise, the frequency response of the microphone and the accompanying electronic equipment is not an important factor as all measurements for a particular run are made at a fixed frequency.

Sound Tube.

The sound tube was made of glass tubing. The tube was selected from a large group because of its lack of taper and its circular cross-section. The radius of the sound tube was chosen as a compromise between the correction necessary to compensate for the tube effect and the highest frequency permitted before other than plane waves would propagate down the tube. As was shown in the previous section the magnitude of the tube attenuation is inversely proportional to the radius, hence a large radius would be desired to minimize the correction for the tube. On the other hand, the smaller the radius the higher the cut-off frequency of the first non-plane mode, hence a higher limit for the usable frequency range of the apparatus. Therefore, a tube radius of .041 cm was chosen. The total length of the sound tube is 120 cm of which approximately 50 cm may be used for measuring attenuations. Each end of the sound tube is terminated with a cone of pyrex wool to eliminate reflections. These terminations and the design of the microphone holder eliminate most reflections; however, at a few isolated frequencies a slight standing wave pattern is observed on the

sound pressure versus distance record. These standing waves are probably due to resonances of the small volumes between the microphone diaphragm and the brass block which holds the microphone.

The elimination of vibrations transmitted from the speaker to the sound tube was one of the most difficult experimental problems to solve. As mentioned in the section on the speaker, a mounting of rubber and tefelon is used to reduce this vibration. However, this mounting was not adequate to eliminate all vibration. Therefore, a rubber link was inserted between the microphone and the section of the sound tube in which the speaker traveled. This link was designed so as not to alter the cross-sectional area of the sound tube and also to maintain the vacuum tightness of the system. It consisted of a rubber washer held in compression and sealed with a rubber sleeve.

Gas Handling System.

In order to insure purity of the gas under test, all connections from the gas source to the sound tube are vacuum tight. This entailed a number of metal to glass seals and metal to metal seals. The former were made by taking a hollow brass cylinder the base of which was drilled to fit a copper tube which was silver soldered to the brass. The copper tubing was placed concentric with the hollow brass cylinder and extended a half inch above the cylinder. The glass tubing

which fitted with approximately .010 inch clearance in the brass cylinder was then sealed in place with Apiezon A black wax. The metal to metal seals were made by converting a standard copper tubing fitting to tighten down on a rubber "O" ring, thus giving a removable vacuum tight seal. A standard gas cylinder is used as the reservoir for CO_2. A 50 ml. glass flask with a stopcock and a tapered joint is used as a reservoir for the liquid CS_2. A specially designed pressure flask made of brass is used for storing the liquid C_2H_4O. The gas handling system consists of three 1000 ml flasks; two are designed for drying the gases and the third is used as a storage flask into which the gases are admitted for mixing. All flasks and gas reservoirs are controlled by appropriate stopcocks or valves and are connected so any one of them may be opened to the sound tube or to the vacuum pumps.

A Welch Duo-Seal mechanical pump is used as a fore pump and a small Distillation Product VMF 5 pump is used as a diffusion pump. During the period of testing the vacuum system, an ionization gauge was used to measure the pressure. Now that the vacuum system is tested, two thermocouple gauges are used to measure the pressure before each gas sample is admitted to the sound tube for test. During the acoustical test, the gas pressure is determined by a Dubrovin Vacuum Gauge for pressures ranging from 1 to 20 mm of Hg. and by a closed end mercury manometer for pressures above 20 mm

of Hg.

Recorder.

The recorder used is a Sound Apparatus Company model
FR. For measurements of large attenuation a 40 decibel po-
tentiometer is employed and for low attenuations a 20 decibel
potentiometer is used. A gear and rack system is used to link
the speaker magnet mechanically to the recorder drive. The
ratio of the distance traveled by the speaker to the distance
the recorder paper moves with respect to the recorder pen
was measured and is checked periodically. The acoustical
response of the recorder was checked and found to be within
the accuracy of the distance measurements.

Electrical Arrangement.

A Hewlett Packard model 205A Audio Signal Generator
is used as the electrical source for the ribbon speaker.
The signal from the generator is amplified by a standard
power amplifier and is fed to the primary of the air core
transformer which serves as a coupling to the speaker. The
sound signal then passes through the gas under test and
is picked up by the condenser microphone. The microphone
signal is then transmitted to a Western Electro-Acoustic
Laboratory Condenser Microphone Complement type 100 B. The
signal then passes through a variable L.C. filter and to a
Hewlett Packard Amplifier model 450 A. The signal is then
fed to the recorder and also to a Hewlett Packard Vacuum

Tube Voltmeter model 400 C, and then to a Du Mont Oscillo-
graph type 208 B.

In order to determine the wavelength of the sound
simultaneously with the measurement of the attenuation co-
efficient, a signal from the microphone and a signal from
the audio generator are put across the vertical and horizon-
tal plates of the oscillograph respectively. The two sig-
nals form an ellipse on the scope screen which opens and
closes as the distance between the speaker and the micro-
phone is varied thus permitting wavelength measurements.

V. EXPERIMENTAL PROCEDURE

The room in which these experiments were made was well insulated and thermostatically controlled to within 2^0 C. The average room temperature during tests was 23^0 C. The entire system, including the sound tube and the gas handling system up to the gas reservoirs, was first evacuated for 48 or more hours. The vacuum was then checked by the thermocouple gauges to insure outgassing had stopped and no leaks were present. The gas to be used was then admitted to the drying flask (in the case of CO_2 and CS_2) or to the drying flask minus drying agent (in the case of C_2H_4O). The gas remained in the drying flask for 48 or more hours during which time the pumps were still on the sound tube. One hour before a run was to be made all electronic equipment was turned on to insure frequency stability of the generator and also to allow the sound tube to come to temperature equilibrium. The gas was then admitted to the sound tube at the minimum pressure for which a signal was obtained sufficiently above the noise level of the system. The gas pressure was then measured and recorded. The signal generator was set at the high limit of the frequency range. The recorder was then started which in turn caused the speaker to move away from the microphone. As the sound pressure versus

distance record was being made, the oscilloscope was watched
and at each closure of the ellipse the record was indexed.
After the speaker had traveled its full distance from the
microphone the recorder was stopped. The recorder motor was
then reversed and another run was made in the opposite di-
rection at the same pressure and frequency. The frequency
of the generator was then lowered and another pair of runs
was made. This continued until the frequency range was
spanned and then the gas pressure was increased and the entire
process repeated. This was continued until the entire fre-
quency over pressure range was covered. These tests were
made in the minimum time possible to reduce any shift in the
absorption curve due to changes in impurities present in the
tube.

The records of the sound pressure versus distance were
then analyzed. The slopes were measured and the distances
between indices were determined. The measured slope, α,
and the wavelength, λ, were tabulated against the correspond-
ing value of pressure and frequency. These data were then
corrected for the tube effect and the classical absorption.
The tube correction was calculated from equation (15) using
the appropriate constants and the corresponding values of
the frequency and pressure. The calculated value was then
multiplied by the experimental factor of 1.045. The clas-
sical correction was determined by inserting the proper gas
constants and the corresponding values of frequency and pres-

sure into equation (2). The two corrections were subtracted from the measured attenuation coefficient leaving the attenuation coefficient of the sound pressure due solely to the phenomena of molecular absorption in decibels per cm. This value was then multiplied by the measured wavelength to give the attenuation per wavelength. In order to compare this value with the theory, the conversion factor from decibels to nepers had to be applied. To convert from pressure attenuation to intensity attenuation a factor of 2 was employed. Therefore, to convert the measured attenuation coefficient to the intensity attenuation per wavelength the following procedure was employed.

$$\alpha_g = \alpha - (\alpha_\eta - \alpha_c) \tag{17}$$

$$\mu = \frac{2 \alpha_g \lambda}{8.686} \tag{18}$$

where α_g = attenuation due to molecular absorption in db/cm
α = attenuation measured experimentally in db/cm
α_τ = attenuation due to the tube in db/cm
α_c = attenuation due to viscosity and heat conduction in db/cm.
λ = measured wavelength in cm
μ = intensity attenuation coefficient per wavelength

The values of μ were then plotted against the logarithm of the ratio of frequency over pressure in kilocycles per atmosphere. These curves will be presented in the next section.

VI. EXPERIMENTAL RESULTS

Tube Effect.

Both air and nitrogen were used to measure the tube
effect as they exhibit only a negligible amount of molecular
absorption in the frequency over pressure range of interest.
The gases were first dried over P_2O_5 for 48 hours, and then
the attenuation coefficient was measured. The procedure used
for these measurements was identical to that described in the
previous section. The classical absorption was subtracted
from the measured attenuation leaving the attenuation due
solely to the tube. Two runs were made for each gas. The
results of these tests were plotted against the ratio of
frequency over pressure in Figures 2 through 5. The best
straight line was drawn through the experimental points.
Averaging the two curves for air, the best straight line is
expressed by

$$\alpha_T = .275 \left(\frac{f}{p} \right)^{\frac{1}{2}} \quad db/cm$$

when f is expressed in kilocycles and p is expressed in mm
of Hg. In order to compare this experimental value with
the theoretical expression, equation (15) must be used

$$\alpha_T = \frac{(\pi \mu c)^{\frac{1}{2}}}{\lambda} \left[\frac{1}{\gamma^{\frac{1}{2}}} + \frac{\gamma-1}{\gamma} \left(\frac{k}{c_p \mu} \right)^{\frac{1}{2}} \right] \left(\frac{f}{p} \right)^{\frac{1}{2}}$$

Tube Attenuation
Dry Air, Run #1

Attenuation (db./cm.)

Frequency/Pressure (Kc./mm. Hg.)

Fig. 2

Tube Attenuation
Dry Air, Run #2

Attenuation (db/cm)

Frequency/Pressure (Kc./mmHg.)

Fig. 3

Fig. 4

Tube Attenuation

Dry Nitrogen, Run #2

Attenuation (db./cm.)

.800
.600
.400
.200
.100
.080
.060
.040

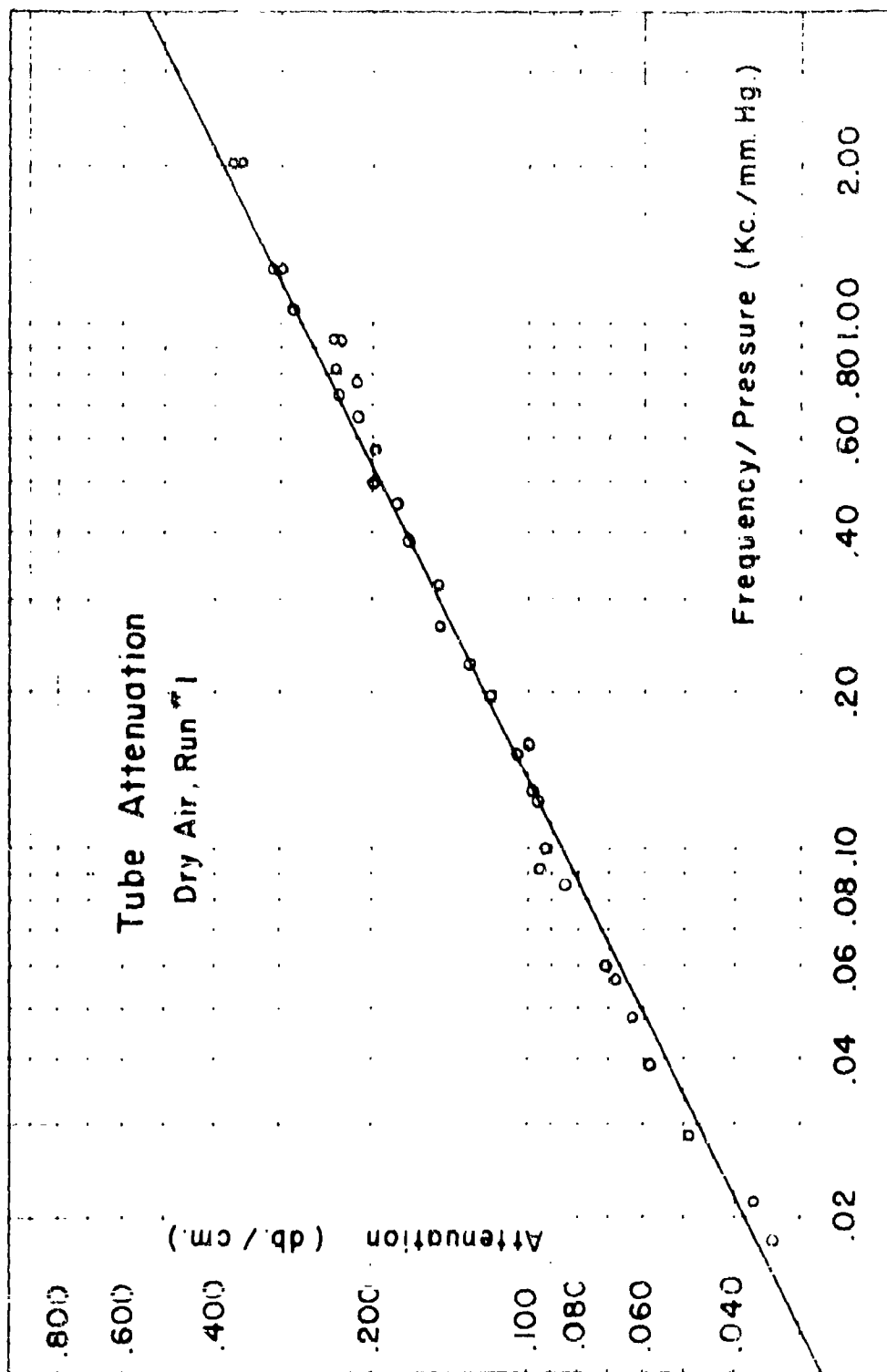Frequency / Pressure (Kc./mm. Hg.)

.02 .04 .06 .08 .10 .20 .40 .60 .80 1.00 2.00
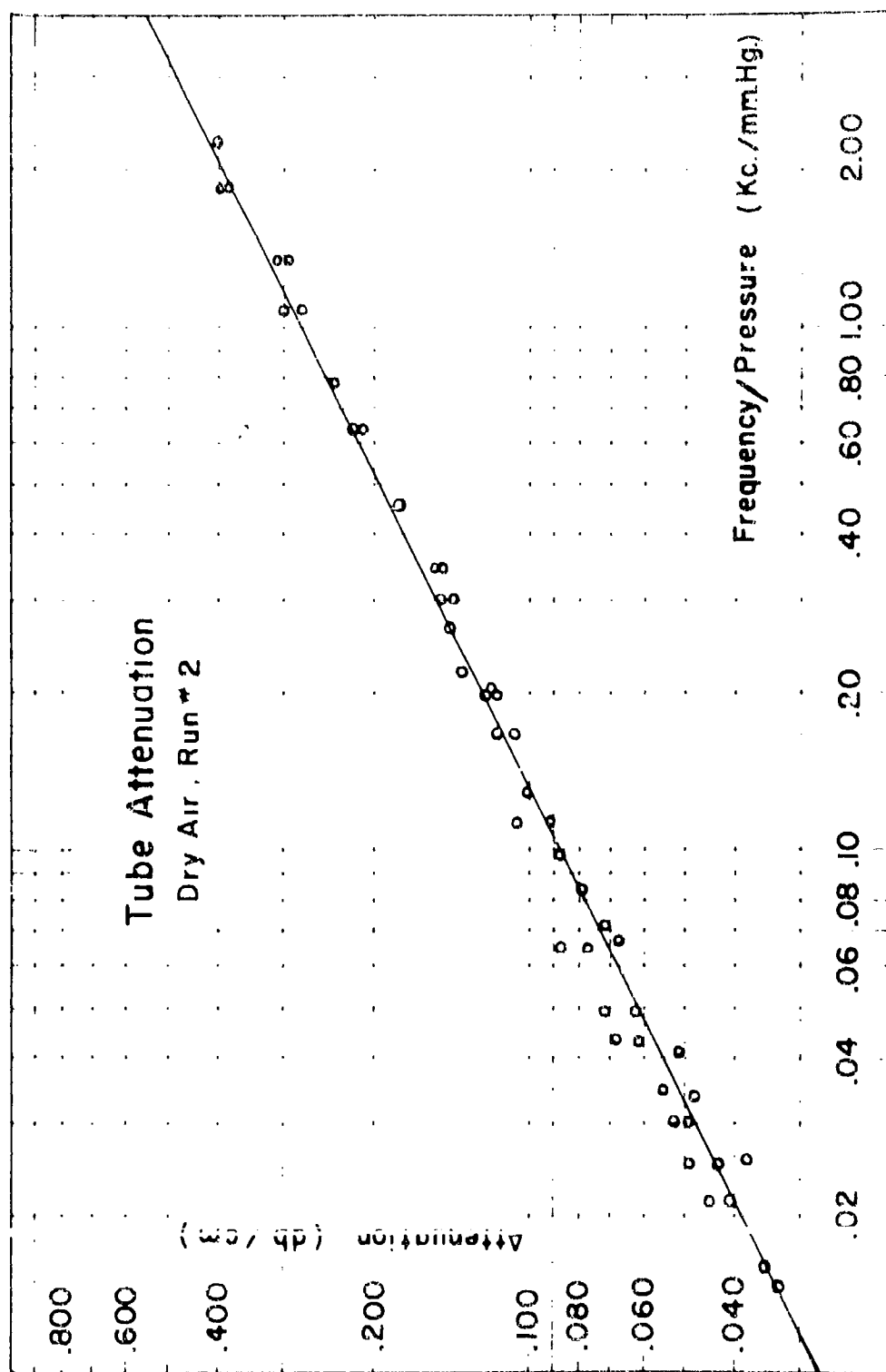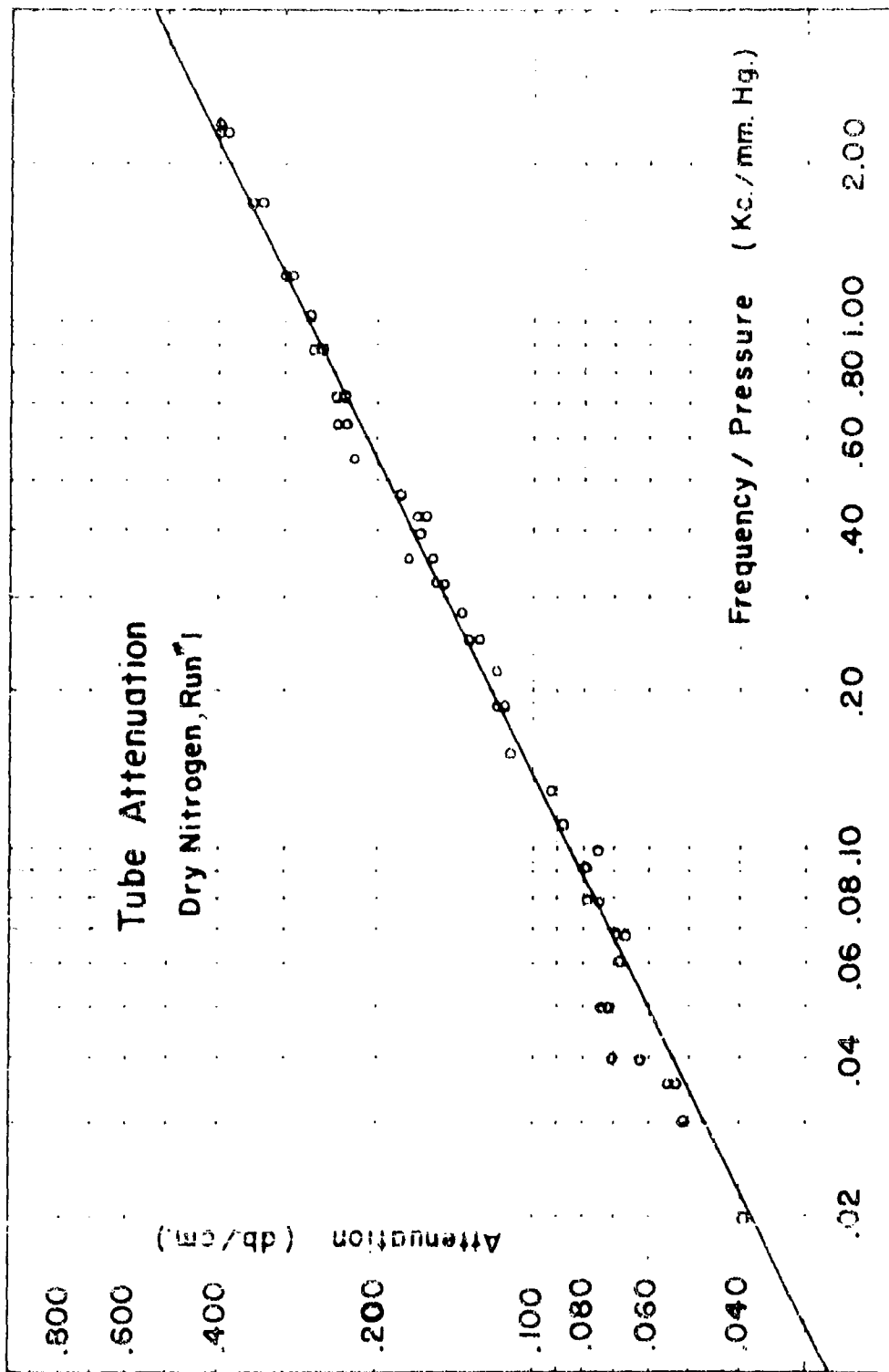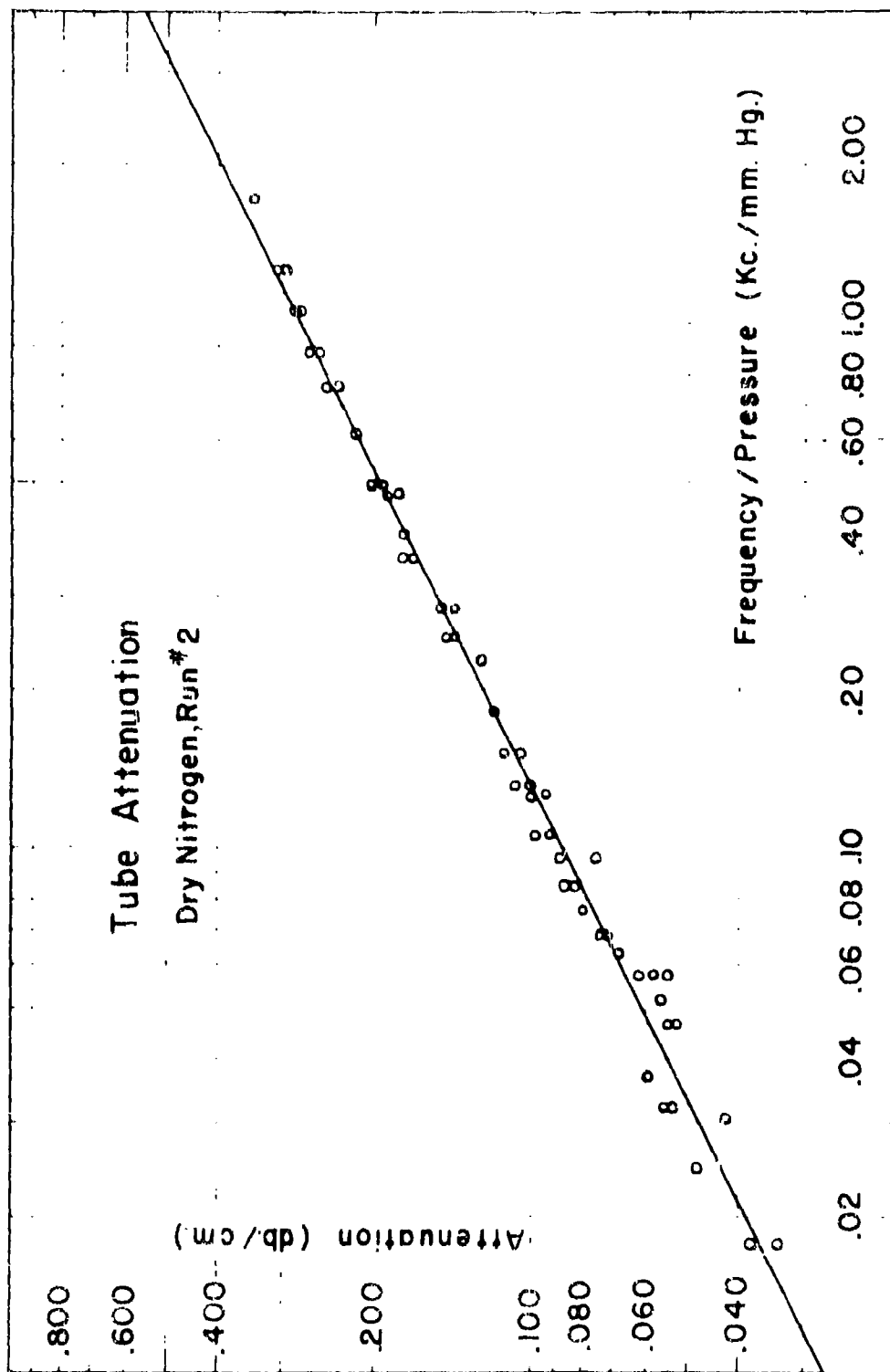
Fig. 5

The constants for air at $23°$ C are

$$K = 56.7 \times 10^{-6} \text{ cal/cm-sec-deg}$$
$$\mu = 182.1 \times 10^{-6} \text{ poises}$$
$$\gamma = 1.403$$
$$C_v = .171 \text{ cal/gm}$$
$$\frac{K}{C_v \mu} = 1.82$$
$$r = .841 \text{ cm}$$

This results in

$$\alpha_{\eta} = .263 \ (f/p)^{1/2} \text{ db/cm}$$

Hence the Kirchhoff equation is low by 4.5% for the glass tube used.

For the case of nitrogen, the expression for the average of the two straight lines is

$$\alpha_{\eta} = .271 \ (f/p)^{1/2} \text{ db/cm}$$

and again, using equation (15) and the following constants for nitrogen at $23°$ C

$$K = 56.7 \times 10^{-6} \text{ cal/cm-sec-deg}$$
$$\mu = 176.5 \times 10^{-6} \text{ poise}$$
$$\gamma = 1.404$$
$$C_v = .176 \text{ cal/gm}$$
$$\frac{K}{C_v \mu} = 1.83$$

one obtains for the calculated tube effect

$$\alpha_{\eta} = .259 \ (f/p)^{1/2} \text{ db/cm}$$

and this is found to be 4.6% lower than the observed value.

As mentioned in the previous discussion of the tube effect, many investigations concerning this problem have been made. The results of these investigations indicate that the Kirchhoff equation is lower than the observed value by a factor ranging from a negligible amount to as much as 15%. Since the magnitude of the tube effect measured by this writer is considerably larger than that measured by the other investigators, it is felt these results are probably more accurate. Consequently, the tube correction used throughout this work was determined by multiplying the value calculated from equation (15) by the experimental factor of 1.045.

Measurements on CO_2.

The CO_2 used was of the commercial grade and was contained in the usual pressure cylinder. The gas pressure was controlled by a regulator which was terminated with a Hoke needle valve. A copper tube was used to connect the cylinder to the CO_2 drying flask. The regulator and copper line were flushed with CO_2 before they were connected to the system. The system up to the regulator was then evacuated. After a sufficient time, CO_2 was admitted to the drying flask which was partially filled with P_2O_5. The CO_2 was allowed to remain in contact with the drying agent for 48 or more hours. During the drying period the flask was periodically rotated

to break up any crusting of the P_2O_5 so as to increase the drying rate.

The dry CO_2 was then admitted to the sound tube and the measurement of attenuation coefficient and wavelength were made. The measured attenuation coefficient was then corrected for the tube effect and for the classical absorption. The tube correction was determined by using equation (15) and the following constants for CO_2 at 23° C.

$$K = 36.6 \times 10^{-6} \text{ cal/cm-sec-deg}$$

$$\mu = 147.1 \times 10^{-6} \text{ poises}$$

$$\gamma = 1.304$$

$$C_v = .157 \text{ cal/gm}$$

$$\frac{K}{C_v \mu} = 1.59$$

After application of the experimental factor of 1.045, the tube correction became

$$\alpha_{\eta} = .234 \ (f/p)^{1/2} \text{ db/cm}$$

where f = frequency in kc
       p = pressure in mm of Hg

The classical correction was calculated from equation (2) using in addition to the constants previously listed

$$M = 44.0 \text{ gm}$$

$$C = 27,000 \text{ cm/sec}$$

$$R = 6.314 \times 10^{7}$$

$$T = 296^\circ \text{ A}$$

thus giving for the classical correction

$$\alpha_c = .00092 \frac{f^2}{p} \ db/cm$$

when f = frequency in kc

p = pressure in mm of Hg.

After all measured attenuation coefficients were corrected, they were converted into the intensity attenuation per wavelength, μ. The values of μ were then plotted against the logarithm of the ratio of frequency over pressure and are shown in Figure 6. The solid curve was determined from Bourgin's expression for a single gas, equation (6)

$$\mu = \frac{2\pi R \Sigma_A C_A \omega}{C_\infty (C_\infty + R)\left[\omega^2 + \Sigma_A^2 \left(1 + \frac{C_A}{C_\infty}\right)\left(1 + \frac{C_A}{C_\infty + R}\right)\right]}$$

using the following constants

$$C_A = 1.869 \ cal/mole$$
$$C_\infty = 4.993 \ cal/mole$$
$$R = 1.986 \ cal/mole$$
$$\Sigma_A = 1.571 \times 10^5 \ sec^{-1}$$

The determination of these constants is explained in the following paragraphs.

In order to determine the con   for equation (6) one must consider the spectroscopic data in the manner discussed in the section on specific heats. The characteristic temperature is determined from the wave number of the mode
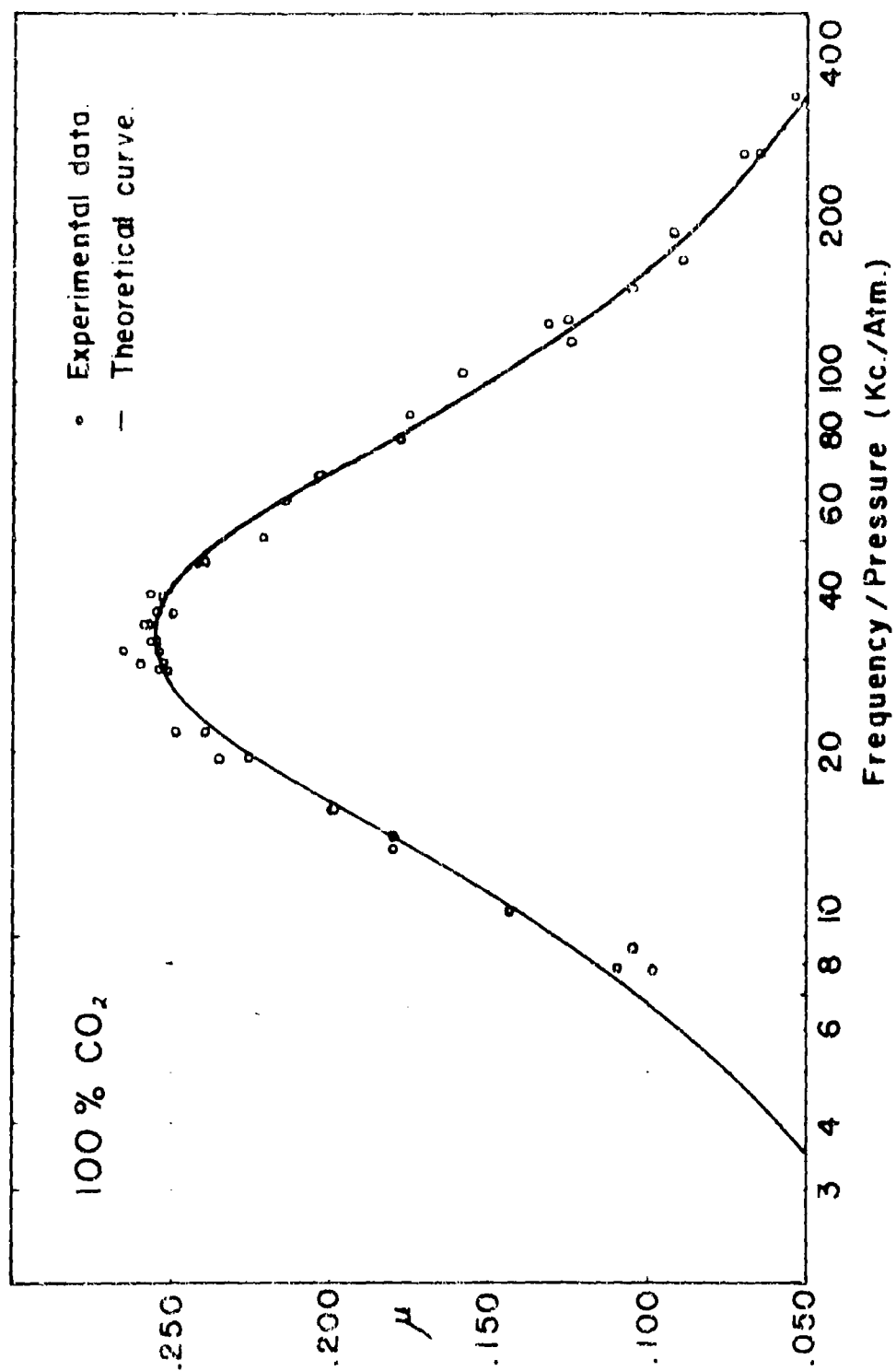
100 % CO₂

Experimental data.
Theoretical curve.

Fig. 6

Frequency / Pressure (Kc./Atm.)

of vibration by

$$\theta = \frac{hc}{k} \nu = 1.439 \, \nu$$

The contribution to the vibrational specific heat for each vibrational mode is determined by equation (13)

$$(C_{vib})_i = p_i R \left(\frac{\theta_i}{T}\right)^2 \frac{e^{-\theta_i/T}}{(1 - e^{-\theta_i/T})^2}$$

The total specific heat at constant volume can then be computed from equation (11). Since CO_2 is a linear molecule, it has only 2 degrees of freedom for rotation. The specific heat at constant volume then is

$$C_v = \frac{5R}{2} + C_{vib}$$

The specific heat at infinite frequency is determined by

$$C_\infty = C_v - C_A$$

where C_A is the vibrational specific heat contributed by those modes of vibration which are activated by the presence of the sound wave. C_A is determined by using the partition function in series form. The series is made up of only those harmonics of a particular mode which are sonically activated. The partition function is then differentiated twice and the resulting expressions are substituted in equation (12). The sum of the contributions of each mode gives the vibrational

specific heat due to the sound wave. Table I shows the results of calculations for CO_2. When the calculated values for the specific heats are put into equation (7) one finds the theoretical value of the maximum attenuation per wavelength to be

$$\mathcal{A}_{max} = .254$$

This calculated value of $\mathcal{A}_{max}$ compares well with the experimental value of Figure 6. To determine the final constant required for equation (6) one must use the experimentally determined frequency of maximum absorption in equation (8)

$$\sum_A = \frac{\mathcal{O}_{max}}{\left[\left(1 + \frac{A}{C_{\infty}}\right)\left(1 + \frac{A}{C_{\infty} + R}\right)\right]^{1/2}} = 1.571 \times 10^5 \; sec^{-1}$$

Now that the value of $\sum_A$ is determined, one can calculate the relaxation time by using equation (4)

$$T_{10}^{A} = \frac{1}{\sum_A}\left(1 + e^{-\theta_A/\varphi}\right) = 6.61 \times 10^{-6} \; sec.$$

In recapitulation the results for CO_2 are as follows:

$$\mathcal{M}_{max} = .255$$

$$f_{max} = 33 \; kc$$

$$\sum_A = 1.571 \times 10^5 \; sec^{-1}$$

$$T_{10}^{A} = 6.61 \times 10^{-6} \; sec$$

The theoretical curve fits the experimental data best if one

44

TABLE I

SPECIFIC HEAT DETERMINATION FOR CO_2

Mode of Vibration (ν)	Wave No. (cm^{-1})	θ (deg)	$(C_{vib})_1$ cal/mole
ν_2	657.3	960.2	1.766
$\frac{1}{2}\nu_2$, $\frac{1}{2}\nu_1$	1285.5	1849.8	.128*
	1388.3	1997.8	
$\frac{1}{2}\nu_2$, $\frac{1}{2}\nu_1$	1932.5	2781	
	2076.5	2988	
ν_3	2349.3	3381	.003
			1.897

$$Q_2 = 1 + 2e^{-\theta_1/T} + \frac{3}{2}\left[e^{-\theta_2/T} + e^{-\theta_3/T}\right] = 1.0828$$

$$Q_1 = 1 + \frac{1}{2}\left[e^{-\theta_2/T} + e^{-\theta_3/T}\right] = 1.00193$$

$C_A = 1.869$ cal/mole
$C_v = 6.862$ cal/mole
$C_\infty = 4.993$ cal/mole

* Contribution due to ν_1 mode only.

assumes the sonically activate vibrational modes are the
first two harmonics of the deformation mode and the funda-
mental of the symmetrical valence mode. It then follows
that

$$C_A = 1.869 \text{ cal/mole}$$
$$C_v = 4.993 \text{ cal/mole}$$

The reproducibility of results for CO_2 was good. The
results for three individual curves for CO_2 were

$$\mu_{max} = .255 \text{ at } 33 \text{ kc}$$
$$\mu_{max} = .253 \text{ at } 37 \text{ kc}$$
$$\mu_{max} = .255 \text{ at } 35 \text{ kc}$$

The value of μ_{max} compares well with that of Leonard
($\mu_{max} = .251$) and of Frick ($\mu_{max} = .249$); however, it is
much higher than that of Fricke ($\mu_{max} = .230$). The probable
reason for this difference is that Fricke measured the at-
tenuation in CO_2 diluted by nitrogen and extrapolated to the
condition of 100% CO_2. Frick has shown this extrapolation
to be in error with a result that the attenuation coeffi-
cients are too low. Since the frequency of maximum absorp-
tion increases at a rapid rate with an increase of impurity,
one would expect a wide variation in f_{max}, with the lowest
value being closest to the true value. The value of f_{max}
measured by Leonard varied from 30 to 45 kc, that measured by

Fricke was 20 kc, and that measured by Frick was 23 kc.

Measurements on CS_2.

The CS_2 used was in the liquid state and was the pur-
est obtainable from the Braun Corporation. It was purified
by vacuum distillation and then dried with P_2O_5. During the
final distillation the vapor was condensed in a 50 ml. flask
which was closed by a stopcock and connected to the test ap-
paratus by a taper joint. Because CS_2 attacks stopcock
grease, rubber, and wax, the vapor was permitted to remain in
the sound tube only long enough for measurements to be made
and was then removed from the system with a roughing pump.
Dow Corning Silicone Vacuum Grease was used in place of the
normally used Apiezon M vacuum grease, for the liquid
reservoir and also for the drying flask where the CS_2 was
held for a considerable time. Although the CS_2 slowly at-
tacked the silicone grease also, it was found the absorption
peak was not affected. The entire system up to the CS_2
reservoir was evacuated for 48 hours. The pressure was then
checked to insure outgassing had stopped and no leaks were
present. The reservoir stopcock was then opened and the CS_2
stopcock was evaporated into the drying flask until the
pressure in the flask was equal to the vapor pressure of CS_2
at 23° C. The vapor was permitted to be in contact with the
P_2O_5 for 48 or more hours. The dried gas was then admitted
to the sound tube and the measurements of attenuation and

wavelength were made.

These data were then corrected in the same manner as those for CO_2. The constants used for CS_2 were:

$$K = 17.4 \times 10^{-6} \text{ cal/cm-sec-deg}$$

$$\mu = 99 \times 10^{-6} \text{ poises}$$

$$C_v = .121 \text{ cal/gm}$$

$$\gamma = 1.28$$

$$\frac{K}{C_v \mu} = 1.45$$

After applying the experimental factor, the tube effect was found to be

$$\alpha_\eta = .189 \ (f/p)^{1/2} \text{ db/cm}$$

where f = frequency in kc
       p = pressure in mm of Hg.

The classical absorption correction was determined from equation (2) using in addition to the constants listed above

$$M = 76.0 \text{ gm}$$

$$C = 20,300 \text{ cm/sec}$$

$$T = 296^\circ \text{ A}$$

thus giving for the classical correction

$$\alpha_c = .00085 \ f^2/p \text{ db/cm}$$

where f = frequency in kc
       p = pressure in mm of Hg.

100% CS₂

μ

Experimental data.
Theoretical curve

Frequency/Pressure (Kc./Atm.)

Fig.7

TABLE II

SPECIFIC HEAT DETERMINATION FOR CS_2

Mode of Vibration (ν)	Wave No. (cm^{-1})	θ (deg)	$(c_{vib})_i$ cal/mole
ν_2	396.7	570.9	2.940
$2\nu_2$	796.0	1145.0	
$3\nu_2$	1190.1	1712.6	
$4\nu_2$	1586.8	2283	
ν_1	656.5	944.7	.905
$2\nu_1$	1313.0	1889.0	
ν_3	1523.0	2192	.066
			3.911

$$Q_2 = 1 + 2e^{-\theta_1/T} + 3e^{-\theta_2/T} + 4e^{-\theta_3/T} = 1.3657$$

$$Q_1 = 1 + e^{-\theta_5/T} + e^{-\theta_6/T} = 1.0428$$

$$C_B = 3.679 \text{ cal/mole}$$
$$C_v = 8.876 \text{ cal/mole}$$
$$C_\infty = 5.197 \text{ cal/mole}$$

With the value of Σ_B determined, the relaxation time may be calculated using equation (5)

$$\tau_{10}{}'' = \frac{1}{\Sigma_B} \left(1 + e^{-\theta_B/T} \right) = .727 \times 10^{-6} \; sec$$

In recapitulation the results for CS_2 are as follows:

$$\alpha_{max} = .382$$
$$f_{max} = 403 \; kc$$
$$\Sigma_B = 1.576 \times 10^6 \; sec^{-1}$$
$$T_{10}{}^B = .727 \times 10^{-6} \; sec$$

The theoretical curve fits the experimental data best if one assumes the sonically activated vibrational modes are the first three harmonics of the deformation mode and the first two harmonics of the symmetrical valence mode. It then follows that

$$C_B = 3.679 \; cal/mole$$
$$C_\alpha = 5.197 \; cal/mole$$

The reproducibility of the results for CS_2 was good. The results of four separate runs were

$$\alpha_{max} = .382 \; at \; 403 \; kc$$
$$\alpha_{max} = .381 \; at \; 402 \; kc$$
$$\alpha_{max} = .387 \; at \; 406 \; kc$$
$$\alpha_{max} = .392 \; at \; 404 \; kc$$

The only other measurements made on CS_2 which could be found in the literature are those of Fricke. His values were μ_{max} = .400 and f_{max} = 379 kc. Because CS_2 was somewhat out of the frequency range of Fricke's equipment, he was able only to measure the absorption coefficient for the lower 1/3 of the curve. This resulted in some uncertainty in his values of the peak height and peak frequency.

Measurements on Mixtures of CO_2 and CS_2.

The gases used were prepared for test in the manner described in the previous two sections. The concentration of each mixture was determined by filling the storage flask to a certain pressure with CO_2 and then CS_2 was added until the final pressure was such as to give the desired concentration. The two gases were allowed to mix by diffusion. The thoroughness of the mixing was checked by periodically taking samples from the storage flask and checking the reproducibility of the measured velocity. It was found approximately one hour was required for adequate mixing of the two gases at room temperature. The mixture was then admitted to the sound tube and the attenuation coefficient and the wavelength were measured for the complete range of frequency over pressure. The tube correction was determined by assuming the wall losses for each gas were proportional to its concentration. Similarly, the classical correction was determined by multiplying the correction for each of the pure gases by their

respective concentrations and taking the sum as the total correction. Measurements were made for concentrations of CO_2 in CS_2 varying from 100% to 0%. The results of these measurements are shown in Figures 8 through 13. The dotted line represents the best fit of Bourgin's theoretical curve to the experimental data, and the solid line is the theoretical curve determined from equation (3). The calculation of the solid curve and a comparison of it with the experimental results will be discussed in a later section. As Figures 8 through 13 show, there is a pronounced shift in peak height and peak frequency as the concentration of CO_2 is reduced. The shift in peak height with concentration of CO_2 is shown in Figure 14, and the shift in peak frequency with concentration of CO_2 is shown in Figure 15.

Measurements on Ethylene Oxide.

In order to make this dissertation more complete, measurements on another mixture of absorptive gases was deemed necessary. To best study the effect of mixtures, the relaxation times of the two gases should be as different as the range of the equipment will permit. Since the relaxation time for CO_2 is such as to cause the absorption peak to fall at the low end of the frequency over pressure range of this equipment, it would be advantageous to choose another gas whose absorption peak would occur near the high end of the frequency over pressure range. Of the gases considered

91.7% CO₂
8.3% CS₂

- Experimental data.
- Theoretical curve.
--- Theor. curve shifted to fit Exp. data

μ

.250 .200 .150 .100 .050

10   20   40   60 80 100   200   400 600   1000

Frequency/Pressure (Kc./Atm.)

Fig. 8

72.6% CO_2
27.4% CS_2

- Experimental data.
- Theoretical curve
- Theor. curve shifted to fit Exp. data.

Frequency/Pressure (Kc./Atm.)

Fig. 9

.300

.250

μ

.200

.150

.100

20 40 60 80 100 200 400 600 1000 2000

- Experimental data.
— Theoretical curve.
--- Theor. curve shifted to fit Exp. data.

66.3 % CO_2
33.7 % CS_2

μ

.300
.250
.200
.150
.100

20 40 60 80 100 200 400 600 1000 2000

Frequency/Pressure (Kc./Atm.)

Fig. 10

49.8% CO_2
50.2% CS_2

° Experimental data.
— Theoretical curve.
--- Theor. curve shifted
    to fit Exp. data.

.350

.300

.250

μ

.200

.150

.100

30   40   60 80 100   200   400 600 1000   2000

Frequency/Pressure (Kc./Atm.)

Fig. 11

Fig. 12

25.2 % CO₂
74.8 % CS₂

Experimental data.
Theoretical curve.
Theor. curve shifted
to fit Exp. data.

Frequency/Pressure (Kc./Atm.)

10.7% CO_2
89.3% CS_2

• Experimental data.
— Theoretical curve.
---Theor. curve shifted
○ to fit Exp. data.

Frequency/Pressure (Kc./Atm.)

Fig.13

μ

.350

.300

.250

.200

.150

20   40   60 80 100   200   400 600 1000   2000

μ_m ∝ Concentration of CO_2 in CS_2

○ Curves included in Thesis
× Additional curves to check reproducibility

Percent CO_2

Fig. 14

f_m vs. Concentration of CO_2 in CS_2

o Curves included in Thesis
x Additional curves to
  check reproducibility

Percent CO_2

Fig.15

f_m (kc.)

500
400
300
200
100
0

for this second mixture, ethylene oxide was chosen because the molecule is more complex than CS_2, thus offering a contrast between the two mixtures, and also since a preliminary test on the gas gave evidence the absorption peak would occur near the high end of the frequency over pressure range.
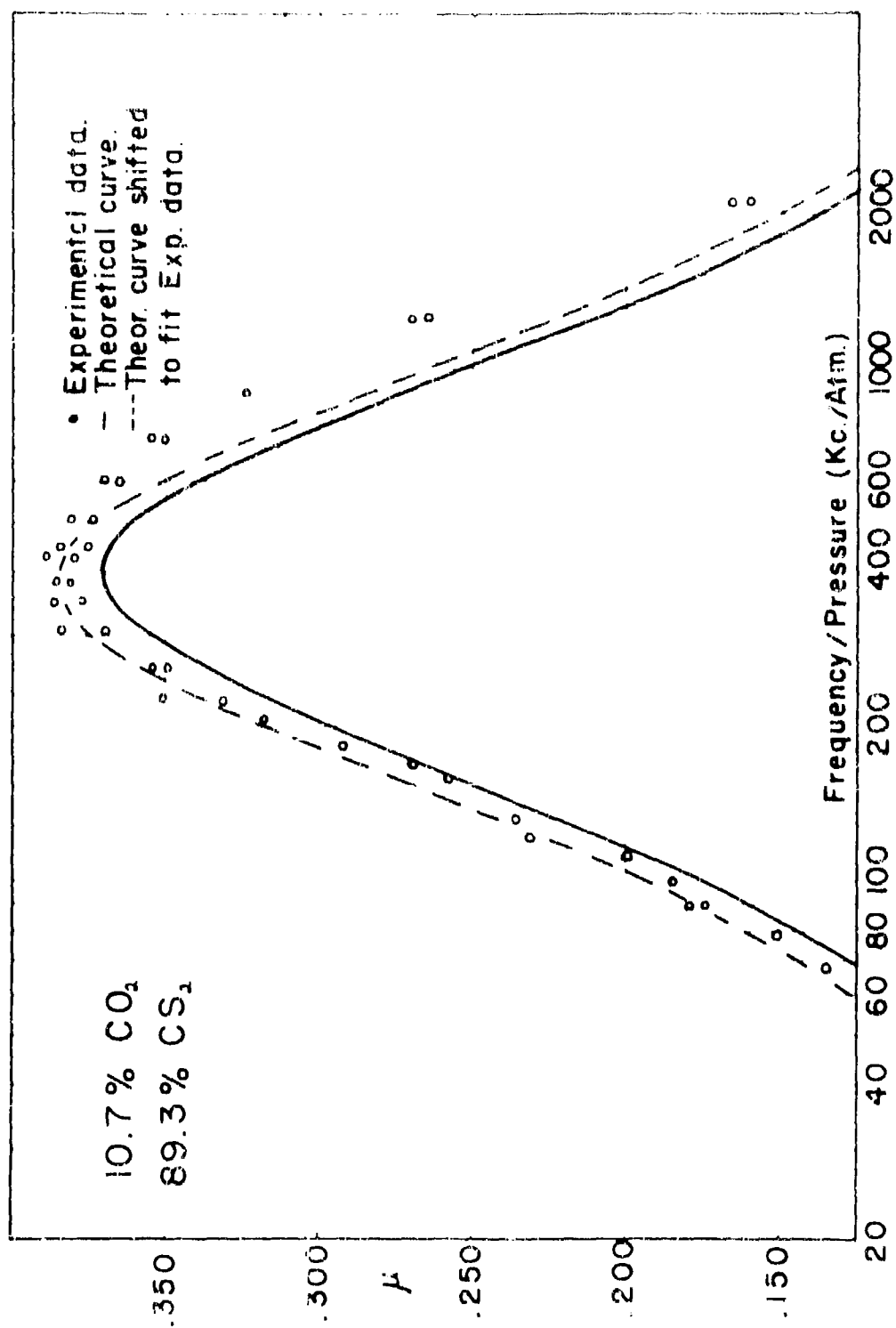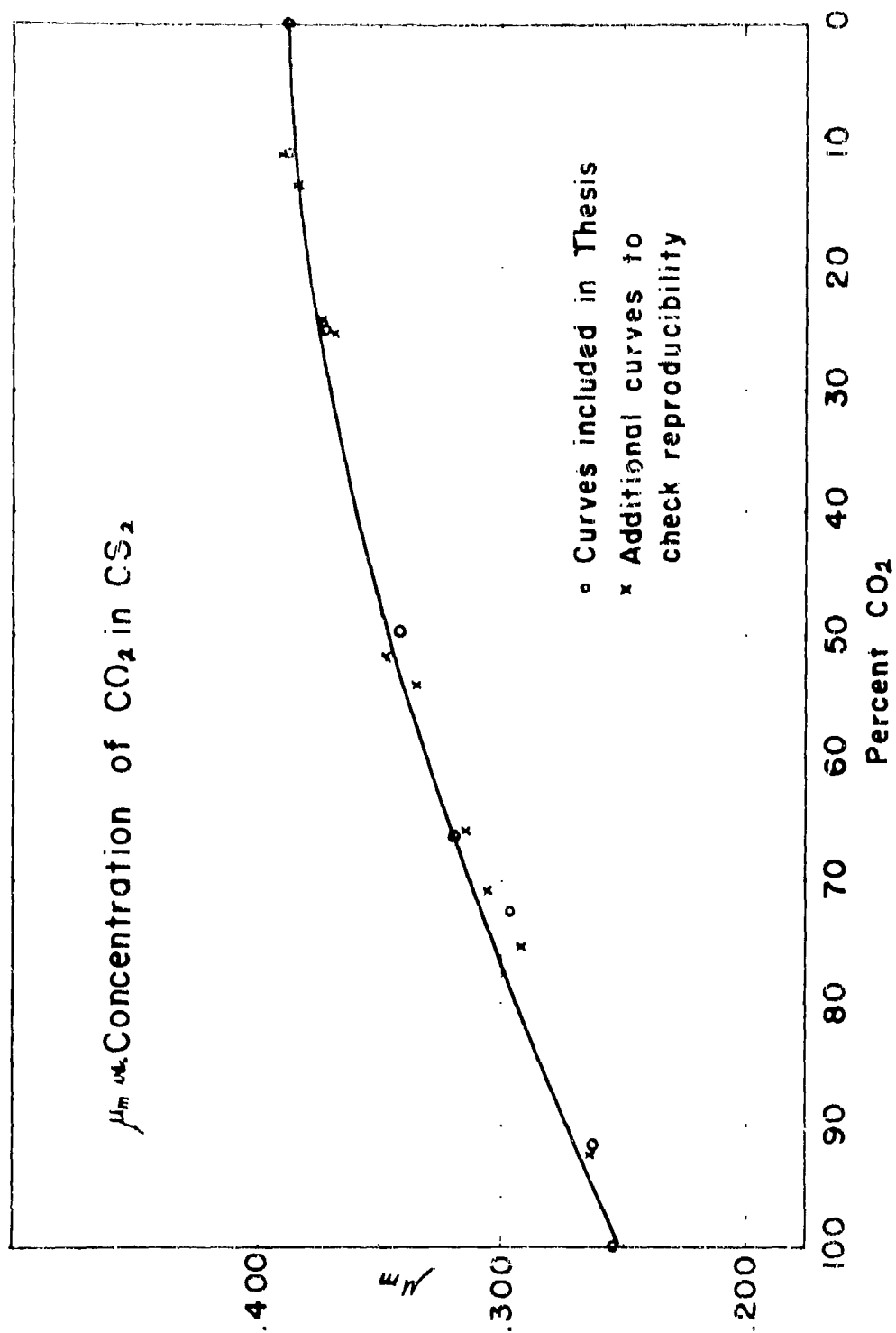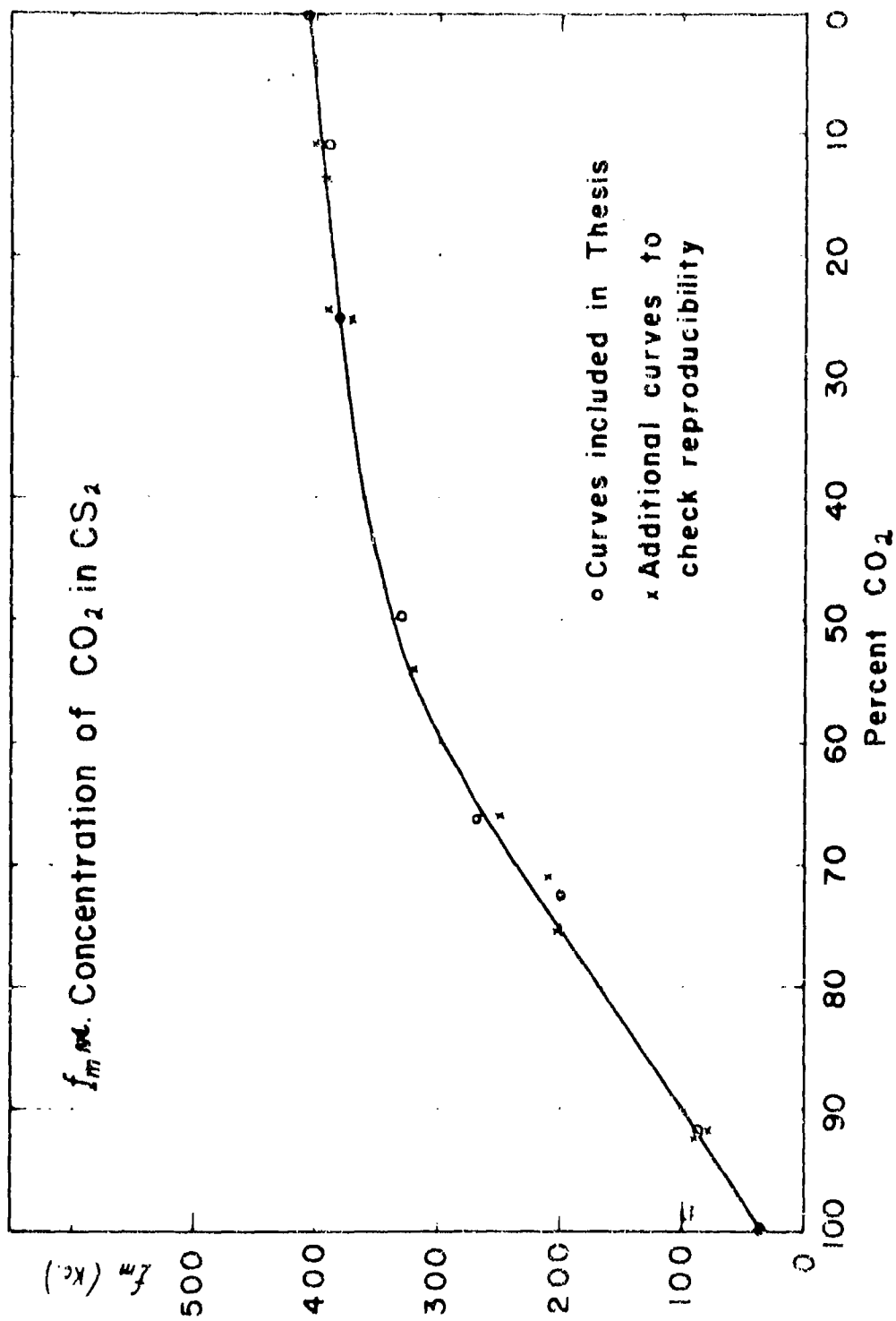
The ethylene oxide used was of the highest purity available from the Eastman Kodak Chemical Company. A more elaborate drying procedure than that used for CO_2 and CS_2 was necessary as the ethylene oxide reacted with all the sufficiently effective drying agents tried. Consequently, the liquid ethylene oxide was further purified by vacuum distillation. A glass manifold was used to which three 50 ml flasks and a specially designed brass pressure cylinder were connected in parallel. The manifold was also connected to a vacuum pump and a mercury manometer. The first flask was filled under vacuum with liquid ethylene oxide. The remainder of the system was evacuated. Flask No. 1, with the ethylene oxide, was cooled to $-78^{\circ}C$ and pumped on for 2 minutes. The pump was closed off and flask No. 2 was cooled to -78° C and flask No. 1 placed at -40° C. The ethylene oxide was allowed to distill over until approximately 1/8 of the original volume remained, then the stopcock of flask No. 1 was closed. Flask No. 2 was pumped on for 2 minutes. Flask No. 3 was cooled to -78° C and flask No. 2 was placed at -40° C. The ethylene oxide was again allowed to distill until 1/3 the volume remained in flask No. 2. Then flask No. 2 was closed

off and the pump was put on flask No. 3 for 2 minutes. The
brass pressure cylinder was next cooled to -78° C and flask
No. 3 was placed at -40° C. The ethylene oxide was again
allowed to distill over until 1/8 of the volume remained in
flask No. 3. The pressure cylinder was closed off and trans-
ferred from the manifold to the acoustic apparatus.

The purified ethylene oxide was then admitted to the
sound tube and the attenuation coefficient and wavelength
were measured. These results were then corrected for the
tube effect and for the classical absorption. The determina-
tion of the constants required for these corrections offered
some difficulty. However, after an extensive literature sur-
vey a value for the heat conductivity of 25.46×10^{-6} cal/cm-
sec-deg was found in Chemical Abstracts 3946 for 1934. The
specific heat at constant pressure of .261 cal/gm was found
in the Journal of Chemical Physics 8,620, 1950. No value
for the viscosity of ethylene oxide vapor could be found.
However, since the viscosity of a gas is dependent on its
molecular structure and size, the viscosity was estimated
by bracketing it between two gases of similar structure and
size. The two gases used were cyclo-propane (C_3H_6) with a
viscosity of 83.5×10^{-6} poise and ethylene (C_2H_4) with a
viscosity of 97.0×10^{-6} poise. Since ethylene oxide is more
similar to the former, a viscosity of 88.0×10^{-6} poise was
decided upon. The ratio of the specific heats was calculated

from the measured sound velocity giving $\gamma = 1.23$. Applying these constants to equation (15) and equation (2), the correction equations for ethylene oxide at 23° C are

$$\alpha_T = .174 \ (f/p)^{1/2} \ db/cm$$

$$\alpha_C = 5.62 \times 10^{-4} \ f^2/p \ db/cm$$

when   f = frequency in kc

       p = pressure in mm of Hg.

All the measured attenuation coefficients were corrected and converted to the intensity attenuation per wavelength. The results for C_2H_4O are shown in Figure 16. The solid curve was determined by using Bourgin's equation (6), where the constants used were

$$C_B = 3.107 \ cal/mole$$

$$C_\alpha = 6.325 \ cal/mole$$

$$R = 1.986 \ cal/mole$$

$$\Sigma_B = 2.90 \times 10^6 \ sec^{-1}$$

The above constants were determined from spectroscopic data in the same manner as was done for CO_2. The ethylene oxide molecule is made up of seven atoms and thus has 21 degrees of freedom. Since it is not a linear molecule, there are 3 degrees of freedom for both rotation and translation. The remaining 15 degrees of freedom are for vibration. Herzberg[24] concludes that in the ethylene oxide molecule, the three heavier atoms form an isosceles triangle and the two
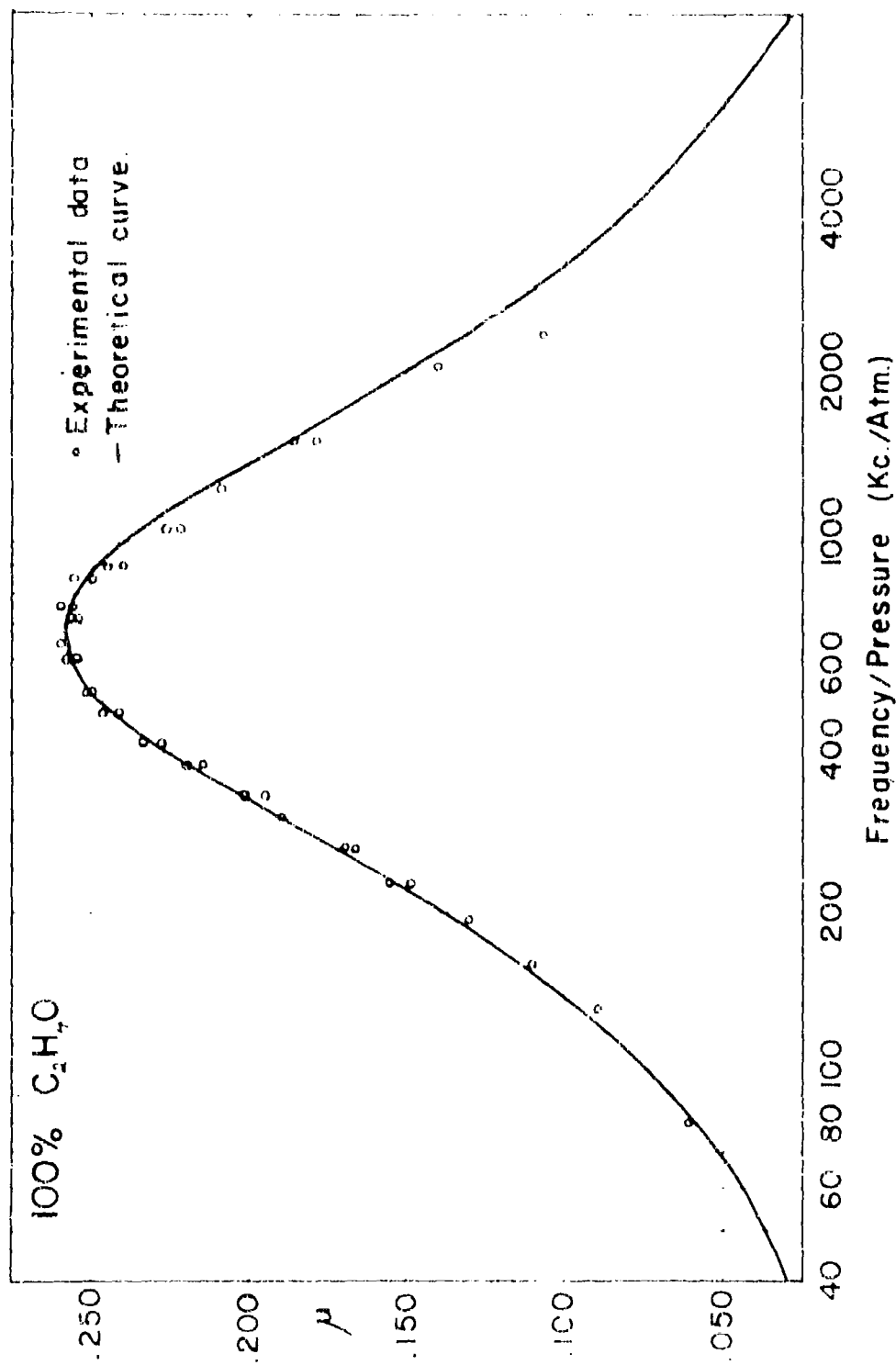
100% C_2H_7O

∘ Experimental data

— Theoretical curve.

Frequency/Pressure (Kc./Atm.)

Fig.16

CH_2 groups form planes at right angle to the C_2O plane. The modes of vibration for ethylene oxide are as follows:

Mode			Wave Number (cm-1)
C-H stretching	V_1 and V_9		3007
	V_0	V_{13}	3061
CH_2 deformation	V_2		1487
	V_{10}		1469
C_2O deformation	V_3		1267
	V_{12}		863
	V_5		806
CH group perpendicular and symmetrical to C_2O plane but bending with respect to yz plane	V_4		1120
	V_{11}		1153
CH groups moving in their plane	V_7		1379
	V_{14}		1153
CH groups twisting with respect to their axis of symmetry	V_8		1023
	V_{15}		704

Table III gives the results of the specific heat calculated for ethylene oxide. When the calculated values for the specific heats are put into equation (7) the theoretical value of the maximum absorption per wavelength is

$$\alpha_{max} = .258$$

The calculated value of α_{max} compares well with the experimental value of Figure 16. To determine the final constant

TABLE III

SPECIFIC HEAT DETERMINATION FOR C_2H_4O

Mode of Vibration (ν)	Wave No. (cm^{-1})	θ (deg)	$(C_{vib})_i$ cal/mole	*
ν_{15}	704	1013	.8114	.7118
ν_5	800	1160	.6303	.5789
ν_{12}	863	1242	.5420	.5108
ν_8	1023	1472	.3448	.3350
ν_4	1120	1612	.2563	.2516
ν_{11}, ν_{14}	1153	1659	.4626	.4524
ν_3	1267	1823	.1600	.1571
ν_7	1379	1984	.1098	.1092
ν_{10}	1469	2114	.0803	
ν_2	1487	2140	.0753	
ν_6, ν_{13}	3000	4327	.0002	
ν_1, ν_9	3061	4405	.0002	
			3.474	3.107

* The contribution to the vibrational specific heat due only to the fundamental of the particular mode of vibration. This value was determined by using the partition function in series form in conjunction with equation (12).

$C_B = 3.107$ cal/mole

$C_v = 9.432$ cal/mole

$C_{vo} = 6.325$ cal/mole

Σ_B required for equation (6) one must use the experimental value of the frequency of maximum absorption in equation (8)

$$\Sigma_B = \frac{\omega_{max}}{\left[\left(1 + \frac{C_B}{C_\infty}\right)\left(1 + \frac{C_B}{C_\infty + R}\right)\right]^{1/2}} = 2.90 \times 10^{6}\ sec^{-1}$$

The relaxation time can now be determined from equation (4)

$$T_{10}^{\ B} = \frac{1}{\Sigma_B}\left(1 + e^{-\theta_B/T}\right) = .356 \times 10^{-6}\ sec$$

In recapitulation, the results for C_2H_4O are as follows:

$$\mu_{max} = .259$$
$$f_{max} = 660\ kc$$
$$\Sigma_B = 2.90 \times 10^{6}\ sec^{-1}$$
$$T_{10}^{\ B} = .356 \times 10^{-6}\ sec$$

The theoretical curve fits the experimental data best if one assumes the sonically activated modes are the fundamental of V_3, V_4, V_5, V_7, V_8, V_{11}, V_{12}, V_{14}, and V_{15}. It then follows that

$$C_B = 3.107\ cal/mole$$

$$C_\alpha = 6.325\ cal/mole$$

The reproducibility of data for C_2H_4O was good. The results of three individual runs were

$\alpha \lambda_{max} = .258$ at 680 kc

$\alpha \lambda_{max} = .260$ at 640 kc

$\alpha \lambda_{max} = .260$ at 660 kc

The literature does not reveal any acoustic measurements made on ethylene oxide; however, W. Griffith[25] measured the vibrational relaxation time of a number of gases by using a steady flow of gas through a jet. He measured the relaxation time for ethylene oxide at 1.23×10^{-6} sec. Considering the accuracy of his method and also the use of the lowest characteristic temperature only in equation (4), the agreement is fairly good.

Measurements on Mixtures of CO_2 and C_2H_4O.

The individual gases were prepared for test as described previously. The concentration of each mixture and the corrections were determined in a similar manner to that used for the CO_2 - CS_2 mixture. The results of measurements made on mixtures of CO_2 and C_2H_4O are shown in Figures 17 through 21. The solid curve was determined from Bourgin's equation (3). As in the case of the other mixture, the peak frequency increases as the concentration of CO_2 is reduced. The peak height is practically constant as the concentration is varied because the absorption of each of the pure gases is almost identical. Figure 22 shows the dependence of the peak frequency on the concentration of CO_2. A

89.9% CO_2
10.1% C_2H_4O

Experimental data
Theoretical curve

Frequency/Pressure (Kc /Atm.)

Fig.17

77.7 % CO_2
22.3 % C_2H_4O

o   Experimental data.
—   Theoretical curve.

Frequency/Pressure (Kc./Atm.)

Fig. 18

49.8% CO_2
50.2% CH_4

μ

.250   .200   .150   .100   .050

20   40   60   80   100   200   400   600   1000   2000

Frequency/Pressure (Kc./Atm)

Fig. 19

28.8% CO_2
71.2% C_2H_4O

- Experimental data
— Theoretical curve

Frequency/Pressure (Kc./Atm.)

Fig. 20

10.8% CO_2
89.2% C_2H_4O

□ Experimental data
— Theoretical curve

Frequency/Pressure (Kc./Atm.)

Fig. 21

f_{max}. Concentration of CO_2 in C_2H_4O

○ Curves included in Thesis.
× Additional curves to check reproducibility.

f_{max} (Kc.)

700 600 500 400 300 200 100

Percent CO_2

90 80 70 60 50 40 30 20 10 0

Fig. 22

comparison of Figure 15 for the CO_2 - CS_2 mixtures with Figure 22 for the CO_2 - C_2H_4O mixtures reveals for the latter mixture a linear dependence of r_{max} on concentration, while for the former mixture the dependence is far from linear.

VII. COMPARISON OF THEORETICAL AND EXPERIMENTAL RESULTS

Figures 6, 7, and 10 show the good agreement between theory and experiment for the pure gases. To make a similar comparison for mixtures of two absorptive gases, equation (3) must be employed. A knowledge of Σ_A and Σ_B are required in order to use equation (3). As mentioned previously, Σ_A and Σ_B are approximately equal to the reciprocal of the relaxation times of gas A and gas B respectively. From a kinetic theory point of view, Σ can be thought of as the transition rate between the excited and the normal state of the molecules. For a mixture of gas A and gas B, the number of transitions per second per unit volume for gas A is given by

$$\Sigma_A = A \, \Gamma_{11} + B \, \Gamma_{12} \tag{19}$$

where   A = number of molecules per unit volume of gas A

      B = number of molecules per unit volume of gas B

$A \, \Gamma_{11}$ = number of transitions per second per unit volume of the A type molecules caused by A-A collisions

$B \, \Gamma_{12}$ = number of transitions per second per unit volume of the A type molecules caused by A-B collisions

Correspondingly, the expression for the transition rate per unit volume for gas B is

$$\Sigma_B = B \, \Gamma_{22} + A \, \Gamma_{21}$$

where $B \, \Gamma_{22}$ = number of transitions per second per unit
volume of the B type molecules caused by B-B
collisions

$A \, \Gamma_{21}$ = number of transitions per second per unit
volume of the B type molecules caused by B-A
collisions

Consequently, to compute Σ_A and Σ_B for various mixtures of gas A and gas B, one must know the value of $A \, \Gamma_{11}$, $B \, \Gamma_{12}$, $B \, \Gamma_{22}$, and $A \, \Gamma_{21}$. For a pure gas, the contribution to the transition rate due to collisions of different type molecules is zero. Therefore, $A \, \Gamma_{11}$, and $B \, \Gamma_{22}$ may be determined from the experimental curves for the pure gases. For a mixture in which gas A is only slightly diluted by gas B, one may consider gas B as an impurity. In such a mixture $A \, \Gamma_{11}$ is the basic transition rate and $B \, \Gamma_{12}$ is the amount contributed to it by collisions of A type molecules with B type.

$CO_2 - CS_2$ Mixture.

As can be seen from Figure 15, f_{max} has approximately a linear dependence on concentration near 100% and 0% CO_2. Consequently, $B \, \Gamma_{12}$ may be evaluated from the experimental curve of 91.6% CO_2 in CS_2. The results of applying the experimental data to equation (8) and (19) show $B \, \Gamma_{12} = 2.74 \times 10^6$. Correspondingly, the experimental data from the 10.7% CO_2 curve and equation (8) and (20) yield $A \, \Gamma_{21} = 1.36 \times 10^6$. These values were then adjusted to allow the maximum

of the theoretical curve for the 49.8% CO_2 mixture to occur at the measured frequency. The adjusted values of the transition rates are

$$\Sigma_A = [.1571x + 2.70 (1-x)] \times 10^6$$

$$\Sigma_B = [1.576(1-x) + 1.20x] \times 10^6$$

where
 $x = A/N$ concentration by volume of CO_2
 $(1-x) = B/N$ concentration by volume of CS_2

Admittedly the above procedure is rather crude; however, it is the only simple method available for determining the required constants.

Using the above expressions for Σ_A and Σ_B in equation (3), the attenuation per wavelength, μ, was calculated for various ratios of frequency over pressure for the various concentrations of CO_2 in CS_2. The results of these calculations are shown as the solid curve in Figures 8 through 13. For each mixture the general shape of the experimental curve compares well with the theoretical. The measured absorption maxima is slightly higher than the calculated values as follows:

%CO_2	Measured μ_{max}	Calculated μ_{max}	% difference
91.7	.261	.247	5.4
72.6	.297	.291	2.0
66.3	.318	.310	2.5
49.8	.343	.328	4.4
25.2	.373	.355	4.8
10.7	.385	.371	3.6

The difference between the absorption measured experimentally and that calculated from Bourgin's general expression (3) is slightly greater than the experimental error which is estimated to be less than 2%.

CO_2 - C_2H_4O Mixture.

In general the experimental data for this mixture were more reproducible and gave smoother curves than for the CO_2 - CS_2 mixture. A possible explanation is the CO_2 -C_2H_4O mixture is less sensitive to slight variations in impurity content.

The transition rates for this mixture were determined in a similar manner to that used for the CO_2 - CS_2 mixture. The experimental data from the 89.9% and 10.8% CO_2 curves were substituted into equations (8), (19) and (20) and yielded $B\Gamma_{12}$ = 3.178 x 10^6 and $A\Gamma_{21}$ = .315 x 10^6. These values were then adjusted to allow the maximum of the theoretical curve for the 49.8% CO_2 mixture to occur at the measured frequency. The adjusted values of the transition rates are

$$\Sigma_A = [.1571x + 2.80 \ (1-x)] \ x \ 10^6$$

$$\Sigma_B = [2.90 \ (1-x) + .315x] \ x \ 10^6$$

Using the above values for Σ_A and Σ_B in equation (3), the attenuation per wavelength, μ, was calculated for various ratios of frequency over pressure for the various

concentrations of CO_2 in C_2H_4O. The results of these calculations are shown as the solid curve in Figures 17 through 21. The agreement between theory and experiment is much better for this mixture than for the CO_2 - CS_2 mixture. The difference between the calculated and the observed attenuation are well within the experimental error.

VIII. CONCLUSIONS

Equipment.

From the performance of the equipment and the data obtained from it, the following conclusions are presented.

1) The tube method may be included in those methods which are capable of measuring the molecular absorption of sound in gases.

2) The apparatus developed has the advantage of:

    a) Accurate control of pressure which shifts the absorption peak to any desired frequency range.

    b) Requiring a relatively small quantity of test gas, thus reducing the gas purification problem.

    c) Producing a sufficiently intense sound field, thus capable of measuring the attenuation in highly absorptive gases.

Experimental Results.

The measurements made of the molecular absorption of sound in gases and in gas mixtures offer the following conclusions:

1) The observed attenuations for pure CO_2, CS_2, and C_2H_4O agree extremely well with the attenuations predicted by Bourgin's theory for a single gas.

2) The observed attenuation for mixtures of CO_2 and CS_2

agree within 2 to 5% with the attenuations pre-
dicted by Bourgin's theory for mixtures of ab-
sorptive gases.

3) For the CO_2 - C_2H_4O mixture, the observed attenua-
tions agree within the experimental error (less
than 2%) with the Bourgin theory.

Measurements of this type yield in addition to the
attenuation coefficient information concerning the collision
parameters of a gas or gas mixture. For example, the number
of collisions required to remove a quantum of vibrational
energy from a molecule and the probability of a transition
occurring due to a single collision can be calculated from
the experimentally determined transition rates, Σ_A and Σ_B.

IX. ACKNOWLEDGEMENT

BIBLIOGRAPHY

BIBLIOGRAPHY

1. Rayleigh, Lord. Theory of Sound. Vol II page 322. (Dover Publication).

2. Neklepajew, N. Ann. d. Physik $\underline{35}$, 175 (1911).

3. Abello, T. P. Proc. Nat. Acad. of Sci. Wash. $\underline{12}$, 699 (1932).

4. Grossmann, E. Ann. d. Physik $\underline{13}$, 681 (1932).

5. Pierce, G. W. Proc. Am. Acad. Sci. $\underline{63}$, 1 (1928); J. Acous. Soc. Am. $\underline{9}$, 185 (1938).

6. Rich, D. L and W. H. Pielemeier. Phys. Rev. $\underline{25}$, 117 (1925).

7. Knudsen, V. O. J. Acous. Soc. Am. $\underline{3}$, 126 (1931); $\underline{5}$, 112 (1933); $\underline{6}$, 199 (1935).

8. Jeans, J. Dynamical Theory of gases (Camb. Univ. Press 1904 Edition).

9. Einstein, A. Sitz. Berl. Akad. 380 (1920).

10. Herzfeld, K and F. O. Rice. Phys. Rev. $\underline{31}$, 691 (1928).

11. Kneser, H. O. Ann. d. Physik $\underline{11}$, 701, 777 (1931).

12. Bourgin, D. G. Phys. Rev. $\underline{34}$, 521 (1929); $\underline{42}$, 721 (1932).

13. Bourgin, D. G. Phys. Rev. $\underline{50}$, 355 (1936).

14. Leonard, R. W. J. Acous. Soc. Am. $\underline{12}$, 241 (1940).

15. Fricke, E. F. J. Acous. Soc. Am. $\underline{12}$, 245 (1940).

16. Frick, R. H. Absorption and Dispersion of Sound in Gases (Thesis UCLA, 1942).

17. Norton, G. A. J. Acous. Soc. Am. $\underline{7}$, 16 (1935).

18. Henry, P. S. H.   Proc. Phys. Soc. **43**, 341 (1931).

19. Fay, R. D.   J. Acous. Soc. Am. 12, 62 (1940).

20. Tischner, H.   Elecktra, Nachr, Tech **7**, 192 (1930).

21. Beranek, L. L.   Acoustic Measurements page 72 (John Wiley and Sons).

22. Waetzmann, E. and W. Wenke.   Akus. Zeits **4**, 1 (1939).

23. Morse, P. M.   Vibration and Sound page 308 (McGraw-Hill Book Co.)

24. Herzberg, G.   Infrared and Raman Spectra (D. Van Nostrand Co., 1945).

25. Griffith, W.   J. Apll. Phys. Dec. 1319 (1950).

A. Government Distribution
   The National Military Establishment

       Research and Development Board
       Pentagon Building
       Washington 25, D. C. (2 copies)

       Department of the Navy

           Chief of Naval Research
           Office of Naval Research
           Washington 25, D. C.
           Attn: Physics Branch (2 copies)

           Director, Naval Research Laboratory
           Washington 20, D. C.
           Attn: Technical Information Officer (9 copies)

       ONR, Branch Offices

           Commanding Officer
           U. S. Navy Office of Naval Research
           Branch Office
           150 Causeway Street
           Boston 10, Massachusetts (1 copy)

           Commanding Officer
           U. S. Navy Office of Naval Research
           Branch Office
           50 Church Street
           New York 7, New York (1 copy)

           Commanding Officer
           U. S. Navy Office of Naval Research
           Branch Office
           American Fore Building
           844 N. Rush Street
           Chicago 11, Illinois (1 copy)

           Commanding Officer
           U. S. Navy Office of Naval Research
           Branch Office
           801 Donahue Street
           San Francisco 24, California (1 copy)

Commanding Officer
U. S. Navy Office of Naval Research
Branch Office
1030 E. Green Street
Pasadena 1, California (1 copy)

Office of the Assistant Naval Attache for Research
Navy No. 100
Fleet Post Office
New York, New York (2 copies)

Director
U. S. Navy Underwater Sound Reference Laboratory
Office of Naval Research
P. O. Box 3629
Orlando, Florida (1 copy)

Director
Naval Research Laboratory
Anacostia Station
Washington 20, D. C.
Attn: Sound Division (1 copy)

Director
U. S. Navy Electronics Laboratory
San Diego 52, California

U. S. Naval Academy
Naval Postgraduate School
Physics Department
Annapolis, Maryland
Attn: L. E. Kinsler (1 copy)

Director
Marine Physical Laboratory
University of California
San Diego 52, California

Director
U. S. Navy Underwater Sound Laboratory
Fort Trumbull
New London, Connecticut (1 copy)

Director
David Taylor Model Basin
Carderock, Maryland
Attn: Sound Section (1 copy)

Director
Ordnance Research Laboratory
Pennsylvania State College
State College, Pennsylvania   (1 copy)

Chief of the Bureau of Ships
Navy Department
Washington 25, D. C.
Attn: Code 330 (1 copy)
        Code 665 (1 copy)
        Code 845 (2 copies)

Naval Medical Research Institute
Naval Medical Center
Bethesda 14, Maryland
Attn: Cdr. D. Goldman NMC (1 copy)

Director, Naval Ordnance Laboratory
White Oaks, Maryland
Attn: Sound Division (1 copy)

Woods Oceanographic Institution
Woods Hole, Massachusetts
Attn: Contract Nobsr 43270 (1 copy)

Department of the Air Forces

        Commanding Officer
        Air Force Cambridge Research Laboratories
        230 Albany Street
        Cambridge 39, Massachusetts
        Attn: Geophysical Research Directorate, ERHS-1

        Director
        National Bureau of Standards
        Division of Mechanics
        Washington 25, D. C.
        Attn: Dr. R. K. Cook (1 copy)

        National Academy of Science
        Committee on Undersea Warfare
        2101 Constitution Avenue
        Washington 25, D. C.
        Attn: Dr. John S. Coleman (1 copy)

B. Non-Government Distribution

        Director
        Laboratory of Acoustic War Research
        Pennsylvania State College
        State College, Pennsylvania (1 copy)

        Massachusetts Institute of Technology
        Acoustics Laboratory
        Cambridge 39, Massachusetts
        Attn: Prof. R. H. Bolt (1 copy)

Harvard University
Cruft Laboratory
Department of Engineering Science and Applied Physics
Cambridge, Massachusetts
Attn: Prof. F. V. Hunt (1 copy)

Catholic University of America
Washington 17, D. C.
Attn: Prof. K. F. Herzfeld (1 copy)

Brown University
Department of Applied Physics
Providence 12, Rhode Island
Attn: Prof. R. B. Lindsay (1 copy)

University of Southern California
Los Angeles 7, California
Attn: Prof. R. E. Vollrath (1 copy)

Norman Bridge Laboratory
California Institute of Technology
Pasadena, California
Attn: Prof. W. G. Cady (1 copy)

University of California
Department of Physics
Los Angeles, California
Attn: Dr. R. W. Leonard (1 copy)

Princeton University
Department of Electrical Engineering
Princeton, New Jersey
Attn: Dr. W. C. Johnson (1 copy)

Case Institute of Technology
Department of Physics
University Circle
Cleveland 6, Ohio
Attn: Dr. R. S. Shankland (1 copy)

Utah University
Salt Lake City, Utah
Attn: Dr. Elsey (1 copy)

Western Reserve University
Department of Chemistry
Cleveland, Ohio
Attn: Dr. F. Hovorka (1 copy)

Note: In those cases where an ONR resident representative has cognizance
of the contract, one copy of the technical report should be sent
to the representative.